Rate and timing cues associated with the cochlear amplifier: Level discrimination based on monaural cross-frequency coincidence detection[a)]

Michael G. Heinz[b)]
Speech and Hearing Sciences Program, Division of Health Sciences and Technology, Massachusetts Institute of Technology, 77 Massachusetts Avenue, Cambridge, Massachusetts 02139 and Hearing Research Center, Biomedical Engineering Department, Boston University, 44 Cummington Street, Boston, Massachusetts 02215

H. Steven Colburn and Laurel H. Carney
Hearing Research Center, Biomedical Engineering Department, Boston University, 44 Cummington Street, Boston, Massachusetts 02215

(Received 1 September 2000; revised 18 July 2001; accepted 23 July 2001)

The perceptual significance of the cochlear amplifier was evaluated by predicting level-discrimination performance based on stochastic auditory-nerve (AN) activity. Performance was calculated for three models of processing: the optimal all-information processor (based on discharge times), the optimal rate-place processor (based on discharge counts), and a monaural coincidence-based processor that uses a non-optimal combination of rate and temporal information. An analytical AN model included compressive magnitude and level-dependent-phase responses associated with the cochlear amplifier, and high-, medium-, and low-spontaneous-rate (SR) fibers with characteristic frequencies (CFs) spanning the AN population. The relative contributions of nonlinear magnitude and nonlinear phase responses to level encoding were compared by using four versions of the model, which included and excluded the nonlinear gain and phase responses in all possible combinations. Nonlinear basilar-membrane (BM) phase responses are robustly encoded in near-CF AN fibers at low frequencies. Strongly compressive BM responses at high frequencies near CF interact with the high thresholds of low-SR AN fibers to produce large dynamic ranges. Coincidence performance based on a narrow range of AN CFs was robust across a wide dynamic range at both low and high frequencies, and matched human performance levels. Coincidence performance based on all CFs demonstrated the ''near-miss'' to Weber's law at low frequencies and the high-frequency ''mid-level bump.'' Monaural coincidence detection is a physiologically realistic mechanism that is extremely general in that it can utilize AN information (average-rate, synchrony, and nonlinear-phase cues) from all SR groups. [DOI: 10.1121/1.1404977]

PACS numbers: 43.66.Ba, 43.64.Bt, 43.66.Fe [MRL]

I. INTRODUCTION

The cochlear amplifier is the name often used to describe an active mechanism within the cochlea that is thought to provide amplification of low-level sounds (Yates, 1995; Moore, 1995). While the mechanism of amplification is not completely understood, several physiological response properties associated with the cochlear amplifier are clear (Ruggero, 1992). The most significant of these is that the active mechanism is vulnerable to cochlear damage and has been shown to be absent in many common forms of sensorineural hearing loss (Patuzzi *et al.*, 1989). This finding raises the question of how the cochlear amplifier benefits normal-hearing listeners, especially in complex listening environments, such as understanding speech in noise, for which hearing-impaired listeners have much difficulty (Moore, 1995). The present study evaluates quantitatively some of the benefits of the cochlear amplifier for extending the dynamic range of the auditory system. The absence of the cochlear amplifier in damaged cochleae is likely responsible for the common report of loudness recruitment by listeners with sensorineural hearing loss and for the associated reduction in dynamic range (see review by Moore, 1995).

It is still not well understood how the auditory system overcomes the dynamic-range problem (for reviews see Evans, 1981; Viemeister, 1988a, 1988b), i.e., the discrepancy between the large dynamic range of human hearing [over 120 dB (Viemeister and Bacon, 1988)], and the limited dynamic range of most auditory-nerve (AN) fibers [less than 30 dB (May and Sachs, 1992)]. A psychophysical experiment in which the dynamic-range problem is clearly evident was examined in the present modeling study: level discrimination of high-level, narrow-band signals in conditions for which information is restricted to frequency regions near the frequency of the signal (e.g., Viemeister, 1974, 1983; Carlyon

[a)]Portions of this work were presented at the Joint Meeting of the Acoustical Society of America and the European Acoustics Association, in Berlin, Germany in 1999.

[b)]Now at: Department of Biomedical Engineering, Johns Hopkins University, 505 Traylor Building, 720 Rutland Avenue, Baltimore, MD 21205; electronic mail: mgheinz@bme.jhu.edu

and Moore, 1984). An influential experiment for level-encoding hypotheses was performed by Viemeister (1983), who found that Weber's law (i.e., constant just-noticeable-difference in level as a function of level) was achieved for high-frequency, narrow-band noise in the presence of band-reject noise. This experiment was designed to prevent the spread of excitation by using a band-reject noise masker and to prevent the use of temporal information by using a high-frequency signal. Viemeister's finding has been taken as evidence that Weber's law must hold in narrow frequency regions and must rely on the use of average-rate information.

Low-spontaneous-rate (LSR), high-threshold AN fibers (Liberman, 1978) have been implicated in the encoding of high sound levels based on average-rate information in narrow frequency regions because of their wide dynamic range (Colburn, 1981; Delgutte, 1987; Viemeister, 1988a, 1988b; Winslow and Sachs, 1988; Winter and Palmer, 1991). However, when models based on cat AN fibers have been used to quantify the total information available in a restricted characteristic-frequency (CF) region with physiological distributions of the SR groups, performance has been predicted to degrade as the level increases above 40 dB SPL (Colburn, 1981; Delgutte, 1987; Viemeister, 1988a, 1988b; Winslow and Sachs, 1988), which is inconsistent with Weber's law and with trends in human performance (Viemeister, 1974, 1983; Carlyon and Moore, 1984). Delgutte (1987) demonstrated that Weber's law could be achieved in single CF-channels by processing high-threshold, LSR AN fibers more efficiently than low-threshold, high-SR (HSR) fibers. He showed that the ''near-miss'' to Weber's law (i.e., a slight improvement in performance as level increases), which is observed in human performance for tones in quiet (e.g., McGill and Goldberg, 1968; Rabinowitz *et al.*, 1976; Jesteadt *et al.*, 1977; Florentine *et al.*, 1987), could be obtained by combining information across CF channels that individually achieved Weber's law. This idea is similar to the assumption made by Florentine and Buus (1981) in their excitation-pattern model.

While there is anatomical evidence that AN fibers with different thresholds and SRs have different patterns of projection to the cochlear nucleus (e.g., Fekete *et al.*, 1984; Rouiller *et al.*, 1986; Liberman, 1991, 1993), there is no strong physiological evidence for the type of preferential processing of LSR fibers used by Delgutte (1987). In addition, the wide dynamic range of LSR fibers depends on the compressive basilar-membrane (BM) responses (Sachs and Abbas, 1974), and there appears to be much less compression at low frequencies than at high frequencies (Cooper and Rhode, 1997; Hicks and Bacon, 1999). Reduced compression at low frequencies is consistent with the absence of nonsaturating (''straight'') rate-level curves at low frequencies in guinea pig (Winter and Palmer, 1991). Thus, it is desirable to investigate other potential sources of information that could produce Weber's law in narrow frequency regions, especially at low frequencies.

The cochlear amplifier is potentially relevant for the encoding of sound level in narrow frequency regions because the associated nonlinear properties influence primarily CFs near the frequency of a tone. Specifically, the nonlinear near-CF response properties include both compressive magnitude responses (Rhode, 1971; Ruggero *et al.*, 1997), as well as level-dependent phase shifts [BM: Ruggero *et al.*, 1997; inner-hair cell (IHC): Cheatham and Dallos, 1998; AN: Anderson *et al.*, 1971]. In evaluating the potential of the cochlear amplifier to extend the dynamic range of the auditory system, it is important to consider several limiting transformations that occur between the BM and the AN. These include (1) saturating rate-level curves (Kiang *et al.*, 1965; Sachs and Abbas, 1974), which act to limit the effect of nonlinear gain on average discharge rate, (2) roll-off of phase-locking at high frequencies (Johnson, 1980; Joris *et al.*, 1994a), which limits nonlinear phase encoding, and (3) randomness of AN responses (Young and Barta, 1986; Miller *et al.*, 1987; Winter and Palmer, 1991; Delgutte, 1996), which limits overall psychophysical performance. Thus, it is important to consider the encoding of information in the AN, not just the compression in BM responses, when evaluating the significance of the cochlear amplifier.

The nonlinear phase changes associated with the cochlear amplifier, which have not been studied in as much detail as the compressive magnitude responses (Sachs and Abbas, 1974; Winter and Palmer, 1991; Moore, 1995; Moore and Oxenham, 1998), are a focus of the present study. These phase cues continue to encode changes in stimulus level at high levels, despite the saturation of average rate above 40 dB SPL for the majority of AN fibers (Sachs and Abbas, 1974; May and Sachs, 1992), and thus may provide a partial solution to the dynamic-range problem. It is important to consider physiologically realistic mechanisms that could make use of the information provided by nonlinear phase shifts. While an absolute phase reference is presumably unavailable to the central nervous system, a relative phase reference can be obtained by comparing across neighboring CFs because the changes in phase are different in adjacent CFs. Carney (1994) demonstrated that nonlinear phase shifts on single AN fibers result in systematic changes in the temporal discharge patterns across CF (i.e., spatio-temporal patterns that vary with level over a wide dynamic range), and hypothesized that changes in spatio-temporal patterns may be important for the encoding of sound level. Any two AN fibers with different CFs have a relative phase difference that varies with level, independent of the absolute phase of the stimulus. Thus, a mechanism that compared the relative timing of two AN fibers would be sensitive to changes in level, without requiring an absolute phase reference.

The present study considers monaural, cross-frequency coincidence detection as a mechanism for decoding the nonlinear phase cues provided by the cochlear amplifier. Coincidence detection is a physiologically realistic mechanism, because any neuron with multiple subthreshold inputs acts as a coincidence detector (Carney, 1994; Joris *et al.*, 1994a). Carney (1990) has shown that several response types in the antero-ventral cochlear nucleus (AVCN) with low CF were sensitive to changes in relative phase across their inputs, consistent with a coincidence detection mechanism. Joris *et al.* (1994a, 1994b) have reported enhanced synchronization in low-CF bushy cells in the AVCN in response to CF tones and in high-CF primary-like-with-notch cells in re-

sponse to low-frequency tones, consistent with coincidence detection at all CFs in globular bushy cells. In addition, there is much evidence for coincidence detection in the binaural system (Yin and Chan, 1990; Goldberg and Brown, 1969; Rose *et al.*, 1966; Yin *et al.*, 1987; Joris *et al.*, 1998). Neurons in the medial superior olive and inferior colliculus have responses that are consistent with coincidence detection between inputs from each ear as a mechanism for decoding interaural time differences that are known to be important for sound localization (reviewed by Colburn, 1996).

In the present study, methods from signal detection theory (SDT) were combined with an analytical nonlinear AN model and a simple coincidence-counting model. Analytical AN models, which represent functional descriptions of neural activity to a well-defined class of stimuli, have been used previously with SDT to evaluate psychophysical performance limits based on the stochastic activity in AN responses (e.g., Siebert, 1965, 1968, 1970; Colburn, 1969, 1973, 1977a, 1977b, 1981). Computational auditory models have also been combined with SDT to evaluate psychophysical performance (e.g., Dau *et al.*, 1996, 1997; Gresham and Collins, 1998; Huettel and Collins, 1999; see Heinz *et al.*, 2001a for review). The present study quantifies the relative contributions of nonlinear magnitude and nonlinear phase responses to level encoding by using four versions of the analytical AN model, which included and excluded the nonlinear gain and nonlinear phase responses in all possible combinations.

II. METHODS

A. Auditory-nerve model

The nonlinear AN model used in the present study is an extension of simple linear analytical AN models used by Siebert (1965, 1968, 1970) and by Colburn (1969, 1973, 1977a, 1977b, 1981). The linear AN model was modified to include the main properties of the cochlear nonlinearities associated with the active process, including (1) nonlinear compressive responses from 30 to 120 dB SPL, (2) compressive nonlinearity restricted to ''near-CF'' regions, (3) compression strength that varies with CF, (4) systematic phase shifts of up to $\pm\pi/2$ above and below CF, (5) no phase shifts at CF, and (6) dynamic range of each SR group that depends on the compressive magnitude response. The response properties of the model are described in the text below, while the assumptions and equations used to specify the model are described in Appendix A. This analytical nonlinear AN model was purposefully kept as simple as possible in order to provide greater intuition and to allow the contribution of each nonlinear property to be investigated separately. The analyses presented below are not limited to this AN model, however, and could be pursued in the future with more complex computational nonlinear models.

The statistics of the AN discharges are modeled by a nonstationary Poisson process with rate function $r(t)$. The phase-locked response of the ith AN fiber (with characteristic frequency CF_i) to a tone burst of level L, frequency f_0, duration T, and phase ϕ, is described by a time-varying rate function similar to that used by Colburn (1981), i.e.,

$$r_i(t;L,f_0,T,\phi) = \frac{\overline{r}[L_{\mathrm{eff}}(L,f_0,\mathrm{CF}_i)]}{I_0\{g[L_{\mathrm{eff}}(L,f_0,\mathrm{CF}_i),f_0]\}} \times \exp\{g[L_{\mathrm{eff}}(L,f_0,\mathrm{CF}_i),f_0] \times \cos[2\pi f_0 t + \theta(L,f_0,\mathrm{CF}_i) + \phi]\}, \quad (1)$$

where $I_0\{g\}$ is the zeroth-order modified Bessel function of the first kind (equal to the time average of the exponential term). Both the average rate $\overline{r}[L_{\mathrm{eff}}]$ and synchrony $g[L_{\mathrm{eff}},f_0]$ are affected by saturating nonlinearities, where the effective level L_{eff} is determined by the nonlinear BM filtering properties and by the level and frequency of the tone. The term $g[L_{\mathrm{eff}},f_0]$ also depends on the stimulus frequency f_0 such that the strength of phase locking decreases at high frequencies. The nonlinear phase response $\theta(L,f_0,\mathrm{CF}_i)$ depends on the level and frequency of the tone as well as on the CF of the AN fiber (see Anderson *et al.*, 1971; Ruggero *et al.*, 1997), and is described similarly to Carney *et al.* (1999). The stimulus is assumed to have random phase ϕ (uniformly distributed) in order to avoid the assumption that the phase of the tone is known to the detector.

Many basic response properties of the AN model are illustrated in Fig. 1. Panels (a)–(c) show the implementation of the nonlinear magnitude responses, which are consistent with physiological data from Ruggero *et al.* (1997). Normalized BM response versus frequency for a 10-kHz CF is shown in Fig. 1(a), for a range of levels. The filters are triangular at low levels, consistent with the linear AN models used by Siebert (1965, 1968, 1970) and Colburn (1969, 1973, 1977a, 1977b, 1981) to fit AN tuning curves in cat. The maximum gain of the cochlear amplifier (i.e., the gain relative to high levels, or equivalently the amount of compression relative to low levels) occurs at CF and is equal to 60 dB for this CF. The nonlinear gain decreases as tone frequency moves away from CF, and the response is linear well away from CF (roughly more than $\pm 1/2$ octaves). Figure 1(b) shows BM output at CF as a function of level for the 10-kHz place. The solid curve represents the nonlinear BM response, while the dashed line represents the linear version of the model. The compressive region extends from 30 to 120 dB SPL, and the model responses are linear below this range. Figure 1(c) shows the cochlear-amplifier gain at CF as a function of CF. The maximum gain decreases as CF decreases, with 60 dB of gain for frequencies above 8 kHz, 20 dB of gain for frequencies below 500 Hz, and a smooth transition for CFs in between. This pattern of nonlinear gain across CF is consistent with both physiological and psychophysical evidence, although the exact amount of gain at low frequencies is still unclear. The majority of BM data has been obtained at high CFs and indicates a maximum gain of roughly 50–60 dB (Ruggero *et al.*, 1997; Nuttall and Dolan, 1996). The BM data at low CFs is less abundant, but indicates reduced nonlinearity at low CFs (e.g., Cooper and Rhode, 1997). Hicks and Bacon (1999) presented psychophysical evidence that cochlear nonlinearity is reduced at low frequencies and is characterized by a gradual, rather than steep, transition as CF decreases.

Figures 1(d) and (f) illustrate how average rate varies

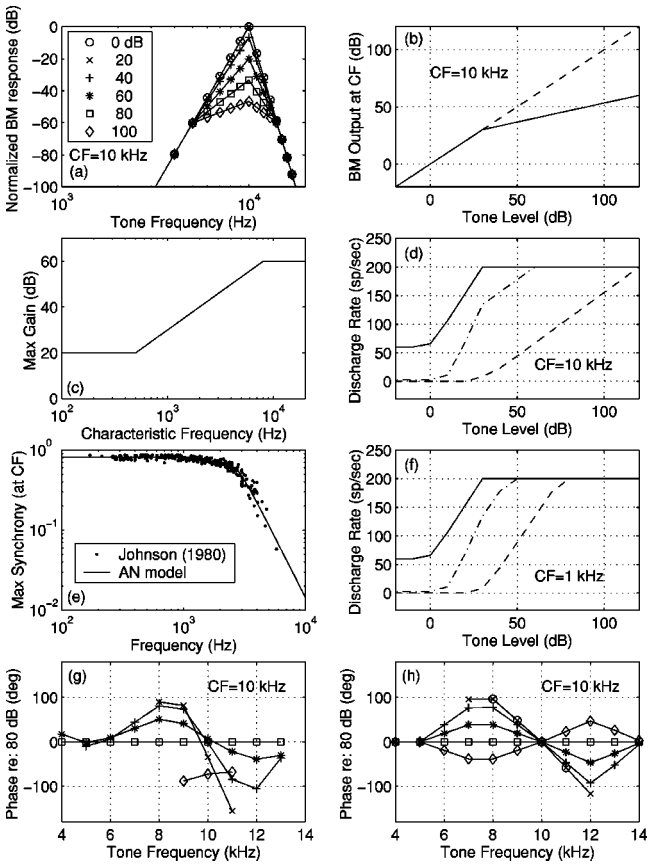

FIG. 1. Nonlinear AN model response properties. (a) Normalized basilar-membrane (BM) response for a 10-kHz place as a function of frequency for levels ranging from 0–100 dB SPL. (b) BM output at CF as a function of level for a 10-kHz place (solid: nonlinear; dashed: linear). (c) Nonlinear gain at CF as a function of CF. (d) Rate-level curves for a 10-kHz tone at CF for three SR groups (HSR: solid, MSR: dashed–dotted, LSR: dashed). (e) Maximum synchrony versus frequency. Model responses are compared to data measured in cat (Johnson, 1980). (f) Rate-level curves for a 1-kHz tone. (g) BM phase-response areas (phase relative to 80 dB SPL) from chinchilla for a 10-kHz CF (data from Ruggero *et al.*, 1997). (h) AN-model phase-response areas for a 10-kHz CF [(g,h): same symbols as in (a)].

with level for the three spontaneous-rate (SR) groups of AN fibers at high and low frequencies, respectively. The AN model represents all fibers within each SR population with a fixed threshold and SR. Based on data from Liberman (1978), SR values of 60, 3, and 0.1 sp/s, thresholds of 0, 10, and 30 dB SPL, and population percentages of 61%, 23%, and 16%, were used for the HSR, medium-SR (MSR), and LSR populations, respectively. A saturated rate of 200 sp/s was used for all three SR groups. Note that the rate-level curves at low frequencies are either ''saturating'' or ''sloping saturating,'' while at high frequencies there is a third class of ''straight'' rate-level curves. This pattern is consistent with rate-level curves in guinea pig described by Winter and Palmer (1991), who found no ''straight'' rate-level curves below 1.5 kHz, and it results from the decrease in cochlear compression as frequency decreases. Figure 1(e) compares the rolloff in phase-locking versus frequency in the model to that in cat (Johnson, 1980).

Figure 1(g) illustrates nonlinear physiological BM phase responses for a 10-kHz CF (Ruggero *et al.*, 1997), while Fig. 1(h) shows the AN-model phase responses. Phase is plotted

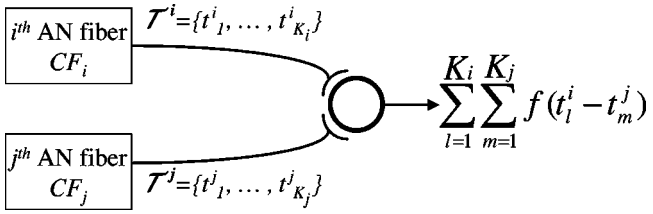

FIG. 2. Simple model of a monaural, cross-frequency coincidence counter. The coincidence detector receives two AN inputs with characteristic frequencies CF_i and CF_j, and discharge times $\mathcal{T}^i=t^i_1,\ldots,t^i_{K_i}$ and $\mathcal{T}^j=t^j_1,\ldots,t^j_{K_j}$, where t^i_l is the lth discharge on the ith AN fiber. The coincidence detector discharges if both inputs discharge within the narrow coincidence window $f(x)$. The output of the coincidence counter is the number of coincidences that occur within the duration of the stimulus.

relative to the phase at a high level (80 dB SPL) in both panels, where each curve represents a different tone level. Thus, any difference from zero represents a phase response that changes with level. The major properties of this nonlinear response, observed for BM responses at high frequencies (Geisler and Rhode, 1982; Ruggero *et al.*, 1997), and IHC (Cheatham and Dallos, 1998) and AN (Anderson *et al.*, 1971) responses at low frequencies, are that (1) phase lags as level increases for $f<\mathrm{CF}$, (2) phase leads as level increases for $f>\mathrm{CF}$, (3) there are no phase changes at CF, (4) the nonlinear-phase region is the same width in frequency as the nonlinear region for the magnitude response, and (5) the maximum phase shifts observed are roughly $\pm\pi/2$ and occur about half way into the nonlinear region. The nonlinear phase responses are consistent with broadened tuning as level increases and the associated changes in the phase-versus-frequency slope (i.e., the slope becomes more shallow as filters broaden).

All predictions in the present study were made with 120 distinct model CFs spaced logarithmically from 300 to 20 000 Hz. It was assumed that the total AN population consists of 30 000 total AN fibers (Rasmussen, 1940) with CFs ranging from 20 to 20 000 Hz (Greenwood, 1990; also see review by Ryugo, 1992). Appendix A describes how the nonlinear-gain and nonlinear-phase properties of the model were included or excluded separately to evaluate the relative contribution of each property to level encoding.

B. Monaural, cross-frequency coincidence counting model

The present study uses a simple coincidence-counting model that was described by Colburn (1969, 1973, 1977a, 1977b) in his studies of binaural phenomena (Fig. 2). A coincidence detector receives two AN-fiber inputs, and is assumed to discharge only when the two input fibers discharge within a narrow temporal window. The output of the coincidence counter is the number of coincident discharges within the duration of the stimulus. The present use of the coincidence-counting model differs from that of Colburn only in the source of the two AN inputs. In the binaural model, each AN fiber was from a different ear and had the same CF. In the present study, the two AN inputs are from the same ear, but can have different CFs. In both studies, performance was assumed to depend only on the number of

coincidences between two AN fibers (i.e., the timing of the coincidences was ignored). The number of coincidences between two AN fibers with discharge times $\mathcal{T}^i=\{t_1^i,\ldots,t_{K_i}^i\}$ and $\mathcal{T}^j=\{t_1^j,\ldots,t_{K_j}^j\}$ is given by

$$\mathcal{C}_{ij}\{\mathcal{T}^i,\mathcal{T}^j\}=\sum_{l=1}^{K_i}\sum_{m=1}^{K_j} f(t_l^i-t_m^j), \tag{2}$$

where t_l^i is the lth discharge out of K_i on the ith AN fiber, and $f(\cdot)$ is a rectangular coincidence window with 10-μs width and unity height (see Colburn, 1969).

C. Evaluation of psychophysical performance limits

1. Optimal processing of AN responses

Psychophysical performance is limited in part by the random nature of AN responses (i.e., different responses are observed for two identical stimulus presentations). Psychophysical performance limits for discrimination experiments have been evaluated with methods from signal detection theory (SDT) by using a nonstationary Poisson process with a time-varying discharge rate $r(t)$ to describe the stochastic nature of AN discharges (e.g., Siebert, 1968, 1970; Colburn, 1969, 1973; Heinz, 2000; Heinz *et al.*, 2001a, 2001b). Heinz *et al.* (2001a) described a general computational method for evaluating psychophysical performance limits using any AN model that describes $r(t)$ for the stimulus conditions of interest. The analytical AN model used in the present study was implemented computationally, and psychophysical performance limits were evaluated based on two hypotheses for the type of information used to perform the task, *all-information* and *rate-place*. The all-information model assumes that the observations used by the optimal processor consist of the complete set of discharge times across the entire AN population, $\mathcal{T}=\{t_l^i\}_{i=1,\ldots,M;l=1,\ldots,K_i}$, where $M=30\,000$ total AN fibers, and K_i is the number of discharges on the ith AN fiber. Thus, the all-information model assumes that the processor makes optimal use of all available information from the AN (e.g., average-rate, synchrony, and phase information). The rate-place model assumes that the optimal processor only uses the number of discharges observed on each AN fiber, $\{K_i\}$.

Optimal performance for single-parameter discrimination experiments can be calculated using a likelihood-ratio test (van Trees, 1968) and has been shown to match the performance limits described by the Cramér–Rao bound (Heinz *et al.*, 2001a). The contribution of each AN fiber to a level discrimination task can be quantified by calculating the normalized sensitivity δ' to changes in stimulus level. [δ' is defined as the sensitivity d' per dB (see Durlach and Braida, 1969; Braida and Durlach, 1988; Heinz *et al.*, 2001a).] The square of the normalized sensitivity of the ith AN fiber in the all-information model is given by

$$(\delta'[\mathrm{CF}_i])^2=\int_0^T \frac{1}{r_i(t)}\left[\frac{\partial r_i(t)}{\partial L}\right]^2 dt, \tag{3}$$

where T is the duration of the stimulus (Siebert, 1970; Heinz *et al.*, 2001a). The total normalized sensitivity based on the population of AN fibers is the sum of the individual normalized sensitivities, $(\delta')^2=\Sigma_i(\delta'[\mathrm{CF}_i])^2$, based on the assumptions of independent AN fibers for deterministic stimuli (Johnson and Kiang, 1976; see also Heinz *et al.*, 2001a), and an optimal combination across AN fibers. The just-noticeable-difference (JND) in level is given by

$$\Delta L=\frac{1}{\sqrt{(\delta')^2}}. \tag{4}$$

Equation (3) describes the normalized sensitivity based on the all-information model; the normalized sensitivity based on rate-place information can be calculated with Eq. (3) by assuming that $r(t)$ is constant across the duration of the stimulus and equal to the average-discharge rate $\bar{r}$ [i.e., setting g to 0 in Eq. (1)]. Thus, the rate-place model does not include information from fine-time or onset responses and therefore predicts inferior performance to the all-information model. The contribution of temporal information in AN discharges can be discerned from a comparison between performance based on the all-information and rate-place models.

2. Performance based on coincidence counts

Performance based on the outputs of a set of coincidence counters was calculated and compared to rate-place, all-information, and human performance. While the all-information predictions represent the optimal performance of any decision device based on the AN discharge times, the coincidence mechanism represents a specific processor that uses the discharge times suboptimally. The number of discharges from a single coincidence detector, $\mathcal{C}_{ij}\{\mathcal{T}^i,\mathcal{T}^j\}$, is a simple function [Eq. (2)] of the two sets of Poisson AN discharge times, $\mathcal{T}^i$ and $\mathcal{T}^j$, and thus the statistics of the coincidence counts can be described (Appendix B). The performance of a single coincidence counter $\mathcal{C}_{ij}$ for level discrimination can be evaluated by calculating the sensitivity index

$$Q_{ij}=\frac{(E[\mathcal{C}_{ij}|L+\Delta L]-E[\mathcal{C}_{ij}|L])^2}{\mathrm{Var}[\mathcal{C}_{ij}|L]}, \tag{5}$$

where the just-noticeable difference for this coincidence counter, $\Delta L_{ij,\mathrm{JND}}$, corresponds to $Q_{ij}=1$. The sensitivity index Q_{ij} represents the commonly used sensitivity index $(d')^2$ if $\mathcal{C}_{ij}$ has a Gaussian distribution with equal variance under both hypotheses, L and $L+\Delta L$ (Green and Swets, 1966; van Trees, 1968). These two assumptions are reasonably accurate for characterizing just-noticeable differences based on a population of independent decision variables (Siebert, 1968, 1970; Colburn, 1969, 1973, 1977a, 1977b, 1981; Heinz *et al.*, 2001a), such as the population of coincidence counts in the present study (see below). Potential deviations from these assumptions do not significantly affect the characterization of performance based on the sensitivity metric Q (Colburn, 1981).

It can be assumed that $E[\mathcal{C}_{ij}|L]$ varies linearly over the incremental level range from L to $L+\Delta L_{\mathrm{JND}}$. Thus, the normalized sensitivity squared for a single coincidence counter, defined as $(\delta'_{ij})^2\triangleq Q_{ij}/(\Delta L)^2$, can be approximated as

$$(\delta'_{ij})^2 \simeq \frac{\left(\frac{\partial}{\partial L} E[C_{ij}|L]\right)^2}{\mathrm{Var}[C_{ij}|L]}. \quad (6)$$

The expectation and variance in Eq. (6) can be evaluated in terms of the stimulus parameters and the two AN CFs (Appendix B). The partial derivative with respect to level in Eq. (6) can be approximated computationally as the difference between the expected value at two slightly different levels divided by the incremental level difference (Heinz *et al.*, 2001a).

The total normalized-sensitivity-squared for a population of coincidence counters is given by the sum of the individual normalized-sensitivities-squared, if it is assumed that the population decision variable is an optimal linear combination of independent (uncorrelated) random variables (or an optimal combination of independent Gaussian random variables). In order to satisfy the independence assumption, it is assumed throughout the present study that no AN fiber innervates more than one coincidence counter. The JND based on coincidence counts is calculated from Eq. (4).

III. RESULTS

A. Distribution of rate, synchrony, and phase information across CF

In order to illustrate the potential benefit of nonlinear phase cues to the encoding of sound level, we first focus on level discrimination at high levels, where the dynamic-range problem is most prominent. Figure 3 illustrates the distribution and relative contributions of rate, synchrony, and phase cues across the AN population of high-spontaneous-rate (HSR) fibers for level discrimination of a 1-kHz, 100-dB SPL tone. The rate responses (i.e., average discharge rate as a function of CF) of the nonlinear-gain, linear-phase model are shown for two tones of slightly different level in panel (b). The more intense tone produces a wider activation pattern; however, the discharge rate for a wide range of CFs near the tone frequency is the same for both tones due to saturation. The distribution of rate information [i.e., normalized sensitivity squared, $(\delta'[\mathrm{CF}])^2$, for the rate-place model] shown in panel (c) illustrates which AN fibers across the population contribute information for level discrimination. The only rate information available for HSR fibers is at frequencies well away from the tone frequency (Siebert, 1965, 1968; also see Stevens and Davis, 1936; Steinberg and Gardner, 1937; Whitfield, 1967).

The situation of primary interest in this study is when information is restricted to AN fibers with CFs near the frequency of the tone. This situation is thought to occur in experiments that use a notched noise masker to limit the spread of excitation (e.g., Viemeister, 1974, 1983; Carlyon and Moore, 1984). A narrow frequency region that will be considered in the current study is indicated by the vertical dotted lines in Fig. 3. This region represents seven model CFs, three above and three below the CF equal to the tone frequency. The narrow frequency region for the 1-kHz tone is 896–1107 Hz and is similar to the notch width used by Carlyon and Moore (1984), which extended ±10% from the

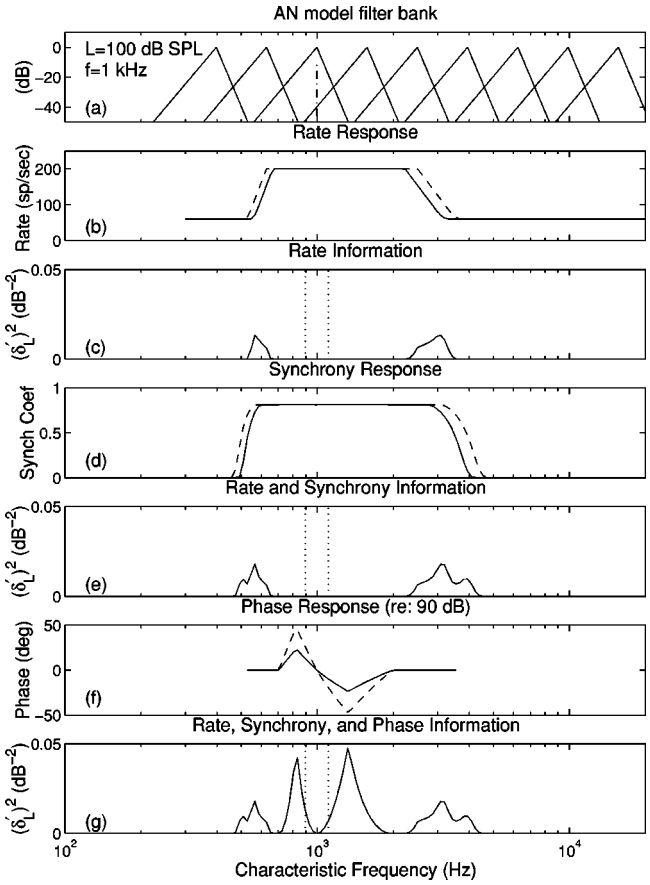

FIG. 3. Distribution of rate, synchrony, and phase information across the AN population of *high-spontaneous-rate fibers* for level discrimination of a low-frequency, high-level tone. (a) AN filter bank with a 1-kHz, 100-dB SPL tone. (b) Average discharge rate as a function of CF for two tones of slightly different level. (c) Average-rate information (normalized sensitivity squared) as a function of CF. The vertical dotted lines indicate the restricted-CF region used in the present study to emphasize the dynamic-range problem. (d) Synchrony coefficient (or vector strength, which ranges from 0 to 1, see Johnson, 1980) as a function of CF for both tones. (e) Information available from both rate and synchrony cues. (f) Normalized phase response (relative to 90 dB) for both tones. (g) Total information from rate, synchrony, and phase cues.

tone frequency. Humans are typically able to perform level discrimination well in the presence of a notched noise (e.g., Viemeister, 1974, 1983; Carlyon and Moore, 1984; Schneider and Parker, 1987); however, Fig. 3(c) shows that there is no average-rate information in HSR AN fibers within the narrow-CF region.

AN phase-locking has a different level dependence than average rate does, and thus it is important to examine the distribution of synchrony information in addition to rate information. Figure 3(d) shows the 1-kHz synchrony coefficient (or vector strength, which ranges from 0 to 1; see Johnson, 1980) for each tone plotted as a function of CF. Synchrony-level curves have thresholds that are roughly 20 dB below rate thresholds, and they typically saturate just above rate threshold (Johnson, 1980). The synchrony-response regions are thus slightly wider than the rate-response regions, but they are also saturated over a wide range of CFs near the tone frequency. The distribution of information available from both rate and synchrony information is shown in panel (e) and represents the all-information

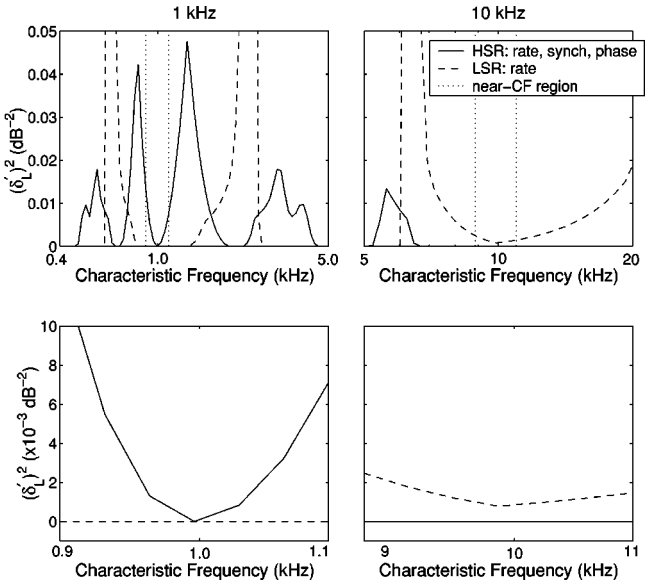

FIG. 4. Comparison of nonlinear phase information in *high-spontaneous-rate (HSR) fibers* and average-rate information in *low-SR fibers* for the encoding of high sound levels in CFs near the tone frequency. The distribution of information across the AN population is shown for level discrimination of 100-dB SPL low- (1 kHz, left column) and high-frequency (10 kHz, right column) tones. The HSR curves (solid) represent rate, synchrony, and phase information, while the LSR curves (dashed) represent only average-rate information. Physiologically realistic properties of HSR and LSR fibers were used to scale the predictions (see text). The vertical dotted lines in the top row represent the narrow-CF region discussed in the present study, which is magnified in the bottom row. Same stimulus conditions were used as in Fig. 3.

normalized sensitivity squared for the nonlinear-gain, linear-phase model. Similar to rate information, there is no synchrony information near the tone frequency for high levels due to saturation of the synchrony coefficient. The useful information from synchrony cues is spread further away from the tone than rate information due to lower synchrony thresholds (Colburn, 1981).

The distribution and relative contribution of nonlinear phase cues is illustrated in panels (f) and (g). The phase responses (relative to the phase at 90 dB SPL) of both tones are shown as a function of CF in panel (f) for the nonlinear-gain, nonlinear-phase model. Auditory-nerve fibers with CFs above and below the tone frequency have phase responses that change with level and thus contribute information. There are no changes in phase at CF, or well away from CF where the BM response is linear. The distribution of the total information provided from rate, synchrony, and phase cues is shown in panel (g), and represents the all-information normalized sensitivity squared for the nonlinear-gain, nonlinear-phase model. By comparing panels (e) and (g), the significant contribution of nonlinear-phase cues to the encoding of level can be seen. While there is no information for the CF equal to the tone frequency, there is significant phase information just below and just above the tone frequency. The amount of phase information is roughly twice as large as the rate and synchrony information. Most importantly for the dynamic-range problem, the only information available in the restricted-CF region is that from nonlinear phase cues.

Figure 4 compares the distribution of information across CF for HSR and LSR fibers at low and high frequencies [see Figs. 1(d) and (f)]. The contribution of nonlinear phase information in HSR fibers is compared to the contribution of average-rate information in LSR fibers. The limited-CF region is indicated by the vertical dotted lines in the top panels, and this region is magnified in the bottom panels. At low frequencies (left column), the HSR fibers (solid curve) contribute significant information from the nonlinear phase cues within the limited CF region. The LSR fibers (dashed curve) do not contribute any information within the limited CF region for the 1-kHz tone because the LSR fibers saturate at 80 dB [see Fig. 1(f)] due to the small amount of compression associated with the cochlear amplifier at low frequencies [Fig. 1(c)]. In contrast, at high frequencies (right column) the HSR fibers contribute no phase information due to the rolloff in phase locking [Fig. 1(e)], while the LSR fibers contribute significant average-rate information within the narrow CF region. The large amount of compression at high frequencies [Fig. 1(c)] results in very shallow (''straight'') rate-level curves for LSR fibers at high frequencies [Fig. 1(d)].

B. Predicted performance based on a narrow CF region

Performance based on a narrow CF region was explored by predicting the JND in level [ΔL; Eq. (4)] using only the information contained in a restricted set of model CFs (seven) surrounding the frequency of the tone. Performance was calculated for a low- (996 Hz) and a high-frequency (9874 Hz) tone, where the tone frequencies were chosen to be equal to one of the 120 model CFs. For the low and high tone frequencies, the near-CF regions used were 896–1107 Hz and 8882–10977 Hz, respectively. Performance was predicted for the HSR, MSR, LSR, and total populations of AN fibers, based on the physiological proportions described by Liberman (1978). Predicted level-discrimination performance is compared for the rate-place and all-information models, where information in the seven model CFs was assumed to be combined optimally, and was scaled to account for the number of AN fibers represented by each model CF. Performance for the monaural-coincidence scheme was calculated based on the same number of total AN fibers as the rate-place and all-information predictions. The seven model CFs in the narrow-frequency region were assumed to innervate a set of four coincidence counters, one of which had both CF inputs equal to the tone frequency. The other three coincidence counters received one CF input above and one below the tone frequency, which were both separated from the tone frequency by an equal number (one, two, or three) model CFs. Based on the assumption that each AN fiber innervates only one coincidence counter, one-half as many same-CF-input coincidence counters were included in the total coincidence population as were coincidence counters with different CF inputs. Thus, rate-place, all-information, and coincidence predictions are all based on the same set of AN fibers with CFs near the tone frequency. Three separate populations of coincidence counters were used associated with the three AN SR groups. This implementation is con-

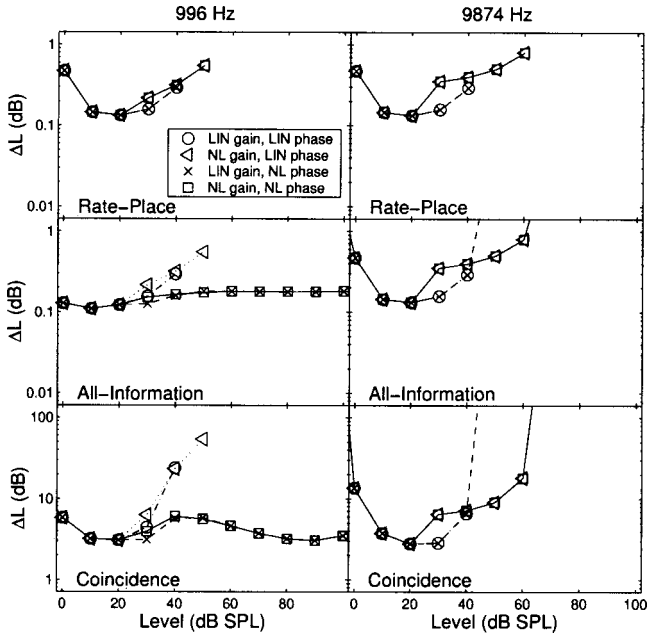

FIG. 5. Level-discrimination performance based on the population of *high-spontaneous-rate (HSR) fibers* in a narrow range of CFs near the tone frequency (see text). The just-noticeable difference ΔL is plotted as a function of stimulus level for a 996 Hz (left column) and a 9874 Hz (right column) tone (500-ms duration). Optimal performance based on average rate and all information is shown in the top and middle rows, respectively. Performance based on a set of monaural coincidence counters is shown in the bottom row. (Note the scale difference between rows.) Four versions of the AN model are shown in each panel to illustrate the effect of nonlinear gain and phase responses. Predictions from the four model versions are identical below 30 dB SPL. Levels for which symbols are not shown represent conditions in which there is no information available for a particular model (i.e., infinite JND).

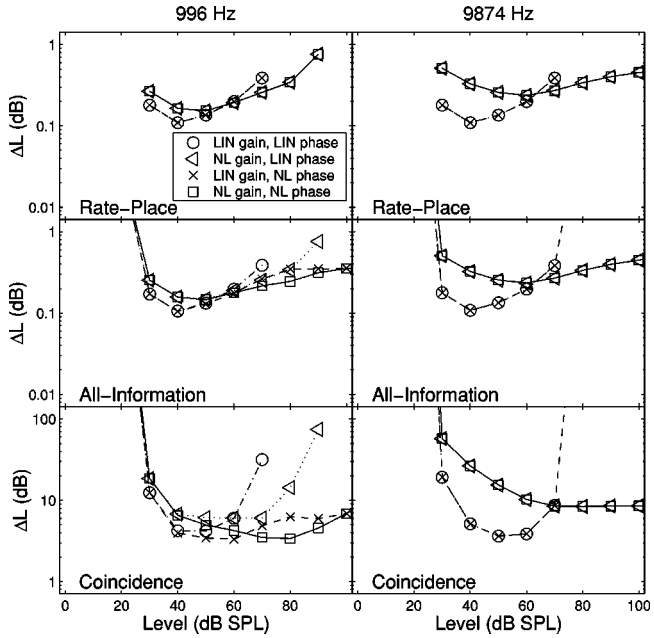

FIG. 6. Level-discrimination performance based on the population of *low-spontaneous-rate (LSR) fibers* in a narrow range of CFs near the tone frequency (see text). The symbols are the same as those used in Fig. 5.

sistent with anatomical studies that have demonstrated distinct projections of the different AN SR groups to the cochlear nucleus (Liberman, 1991, 1993).

Figure 5 shows level-discrimination performance based on the HSR fibers within the narrow frequency region in terms of ΔL as a function of stimulus level L for a low-frequency (left column) and a high-frequency (right column) tone. Rate-place, all-information, and coincidence performance are shown in the top, middle, and bottom panels, respectively. Note that the scale for the ordinate of the coincidence panel is different than those for the rate-place and all-information panels. In order to illustrate the relative contributions from nonlinear-gain and nonlinear-phase properties, performance based on four versions of the AN model is shown in each panel.

Average-rate information in HSR fibers encodes changes in level only over a limited dynamic range (Fig. 5, top row). When the nonlinear gain is included in the AN model, the dynamic range over which changes in level are encoded is extended by 10 dB at low frequencies and by 20 dB at high frequencies. The degradation in performance at 30 dB SPL for the nonlinear-gain models results from the compressive BM response that begins at 30 dB SPL [Fig. 1(b)]. The larger influence of the nonlinear gain at high frequencies compared with low frequencies is due to the CF dependence of the cochlear-amplifier gain.

The contributions of synchrony and nonlinear-phase information are demonstrated by comparing rate-place and all-information predictions (Fig. 5, top and middle rows). The role of synchrony information is most clearly illustrated with the linear-phase versions of the AN model. Synchrony information improves performance at low levels for the low-frequency tone; however, synchrony does not extend the dynamic range to higher levels due to the saturation of synchrony coefficients at lower levels than average rate (Colburn, 1981). The nonlinear phase responses extend the dynamic range for level discrimination up to at least 100 dB SPL at low frequencies. This is in sharp contrast to the range of rate-place information, which does not encode level changes in HSR fibers above 50 dB SPL. At high frequencies, rate-place and all-information predictions are essentially the same because of the sharp rolloff of phase-locking at high frequencies [Fig. 1(e)].

The predictions from the simple coincidence-counter model (Fig. 5, bottom row) follow the same general trends as the all-information predictions for both low and high frequencies, but are more than an order of magnitude worse than optimal all-information performance. The coincidence model utilizes the average-rate (and some of the synchrony) information that dominates performance below 30 dB SPL. The coincidence mechanism also successfully utilizes nonlinear phase cues provided by the cochlear amplifier at low frequencies.

Predictions based on the set of LSR AN fibers within the narrow frequency region are shown in Fig. 6. At both low and high frequencies, the nonlinear gain extends the dynamic range over which changes in level are encoded for the rate-place model; however, performance degrades significantly above 40 dB SPL at low frequencies. Changes in level of a 1-kHz tone are not encoded above 90 dB SPL in the average rate of the set of LSR fibers with CFs near the frequency of the tone. In contrast, LSR rate-place performance for a high-

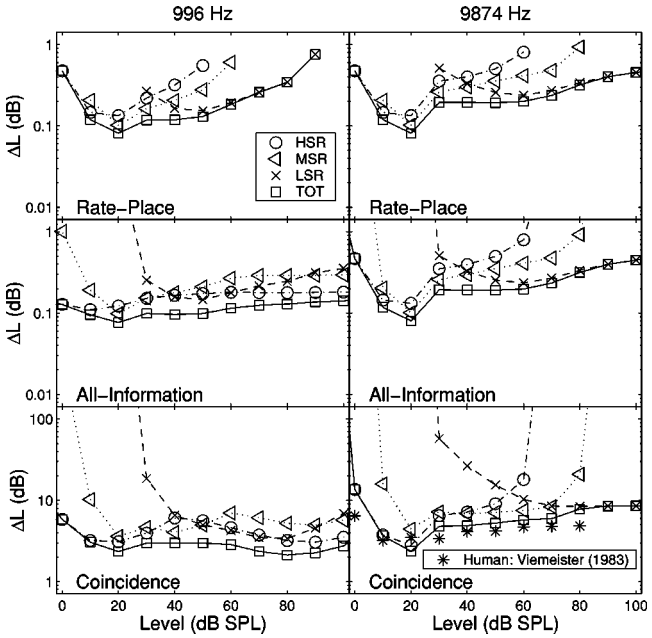

FIG. 7. Level-discrimination performance based on individual and combined spontaneous-rate groups in a narrow range of CFs near the tone frequency (see text). The just-noticeable difference ΔL for the nonlinear-gain, nonlinear-phase AN model is plotted as a function of stimulus level for a 996 Hz (left column) and a 9874 Hz (right column) tone (500-ms duration). Optimal performance based on average rate and all information is shown in the top and middle rows, respectively. Performance based on a set of monaural coincidence counters is shown in the bottom row. (Note the scale difference between rows.) HSR: high-spontaneous-rate; MSR: medium-spontaneous-rate; LSR: low-spontaneous-rate; TOT: optimal combination of all three SR groups. Levels for which symbols are not shown represent conditions in which there is no information available (i.e., infinite JND). Human data for level discrimination of a 200-ms high-frequency noise band (6–14 kHz) in the presence of a notched noise is shown by the stars in the bottom right panel (Viemeister, 1983).

frequency tone is roughly constant across a wide dynamic range, up to 100 dB SPL. The all-information predictions demonstrate that the nonlinear phase responses extend the dynamic range of LSR fibers at low frequencies up to 100 dB SPL. The coincidence predictions (Fig. 6, bottom row) at low frequencies show a small benefit from the nonlinear gain responses; however, performance based on nonlinear gain alone significantly degrades above 70 dB SPL. The benefit from the nonlinear-phase cues is also seen in performance based on the coincidence counters, extending the dynamic range beyond that based on nonlinear gain alone. At high frequencies, coincidence performance is constant above 70 dB SPL when the nonlinear gain is included in the AN model.

The contribution of each of the three SR groups to level-discrimination performance based on the narrow range of CFs is shown in Fig. 7 for both low- and high-frequency tones. The rate-place predictions illustrate that the HSR and MSR fibers are primarily responsible for performance at low levels, while the LSR fibers are responsible at high levels (roughly above 50 dB SPL at both low and high frequencies). Performance based on the combination of average-rate information in the three SR groups degrades by an order of magnitude between 20 and 90 dB SPL at low frequencies, and no changes in level are encoded above 90 dB SPL (see also Colburn, 1981; Delgutte, 1987). Changes in level are encoded much more consistently across level at high frequencies as a result of the large amount of cochlear compression at high frequencies.

The all-information predictions (Fig. 7, middle row) based on all three SR groups are roughly constant across a dynamic range of 100 dB at low frequencies, unlike the rate-place predictions. Thus, Weber's law is achieved based on information within a narrow range of CFs at low frequencies only when nonlinear-phase information is included. Furthermore, performance based on the HSR fibers is as good and often better than performance based on the MSR and LSR fibers for low frequencies, especially at high levels.

Performance at low frequencies based on the populations of coincidence counters (Fig. 7, bottom left panel) demonstrates roughly the same pattern as the all-information predictions, but is roughly an order of magnitude worse than optimal performance. Performance is roughly constant across a wide dynamic range and is primarily determined by the HSR fibers. At high frequencies, performance based on the coincidence counters is also roughly constant from 10 to 100 dB SPL and is determined by HSR fibers at low levels, by MSR fibers at medium levels, and by LSR fibers at high levels. For comparison, human performance for level discrimination of a high-frequency, bandpass noise (6–14 kHz) in a noise masker with a 6–14 kHz notch is shown by the stars (Viemeister, 1983).

C. Predicted performance based on entire population (all CFs)

Predicted performance based on the entire population of AN fibers (i.e., all CFs) was compared to human performance in a pure-tone level-discrimination task in quiet. Rate-place and all-information predictions [Eq. (4)] were based on the optimal combination of information from the 120 model CFs. The same four coincidence counters were used for each CF as in the narrow-CF predictions described above. The total normalized sensitivity squared was the sum of the individual normalized-sensitivities-squared from each of the four coincidence counters at each of the 120 model CFs.[1] In this implementation, each AN fiber innervated only one coincidence counter, and thus the normalized-sensitivities-squared could be summed based on the assumption of independent AN fibers.

Predicted rate-place, all-information, and coincidence performance based on the entire HSR population is shown in Fig. 8 for low- and high-frequency, 500-ms tones. Rate-place performance (top row) based on the linear AN model is flat above 20 dB SPL for the low-frequency tone, consistent with the predictions of Weber's law based on the spread of excitation (Siebert, 1968). For the high-frequency tone, there is a small rise in ΔL above 60 dB SPL for the linear AN model. This rise is due to the upper side of the excitation spreading beyond the highest CF, and it is consistent with the expected $\sqrt{2}$ reduction in ΔL due to the loss of one-half of the information. There is only a small effect of nonlinear gain on rate-place performance based on the population of CFs. The degradation in performance for the high-frequency tone at mid-levels results from the large amount of compression at

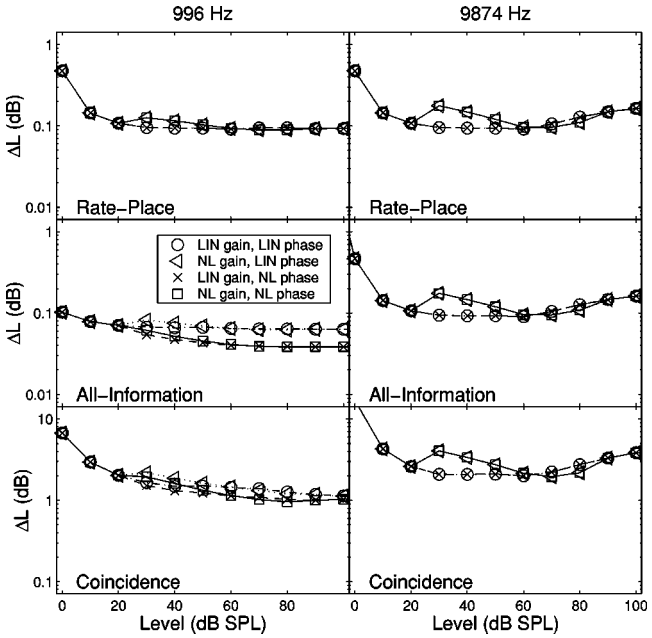

FIG. 8. Level-discrimination performance based on the total population of *high-spontaneous-rate (HSR) fibers*. The symbols are the same as those used in Fig. 5.

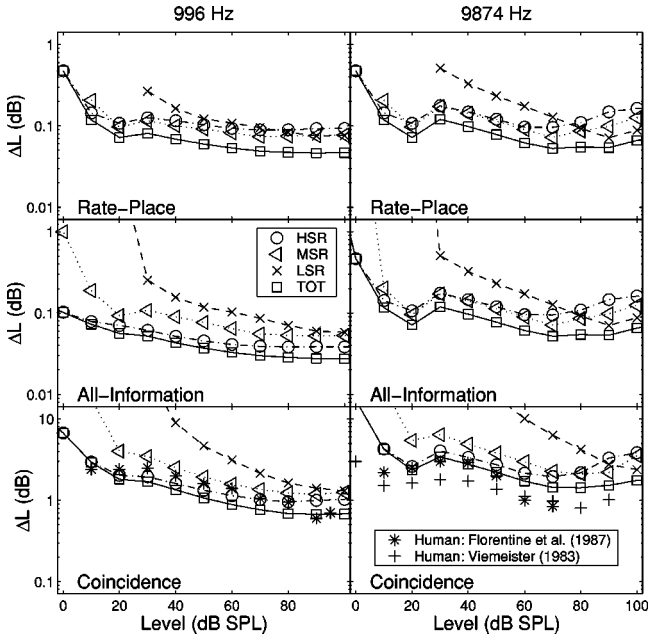

FIG. 9. Level-discrimination performance based on the total population of individual and combined spontaneous-rate groups (same symbols as Fig. 7). Human data for level discrimination of 500-ms tones measured as a function of sensation level is shown by the stars in the bottom left and right panels (Florentine *et al.*, 1987). Human level–discrimination data for a 200-ms high-frequency noise band (6–14 kHz) in quiet is shown by the plus symbols in the bottom right panel (Viemeister, 1983).

high frequencies. The presence of a mid-level bump at high, but not low, frequencies is consistent with human performance (Florentine *et al.*, 1987). At low frequencies, synchrony improves all-information performance (Fig. 8, middle row) for the linear AN model by a factor of five at 0 dB SPL, and by a factor of slightly less than two for higher levels. Weber's law is again predicted above 20 dB SPL based on the contributions of rate and synchrony information.

The near-miss to Weber's law is present in the low-frequency predictions when the nonlinear phase responses are included in the AN model. This is consistent with the nonlinear phase responses producing Weber's law within narrow-CF regions (Fig. 5), and the combination of information across CFs producing the near-miss to Weber's law. Predicted trends based on the population of coincidence counters (Fig. 8, lower row) generally resemble the all-information predictions at both low and high frequencies, with the exception that the benefit from synchrony information at very low levels is not observed. Overall, nonlinear gain and nonlinear phase have only a small effect on predicted level-discrimination performance in quiet due to spread of excitation, which is dominated by *linear*, off-CF responses.

The contribution of the three SR groups to the predicted performance based on the total AN population is shown in Fig. 9 for the nonlinear AN model. The rate-place predictions for the low-frequency tone demonstrate that each of the three SR groups contribute essentially equally above 50 dB SPL. Performance based on the total population of AN fibers (squares) decreases only slightly between 30 and 80 dB SPL. Rate-place predictions at high frequencies show that both the HSR and MSR population have a mid-level bump, while the LSR population does not. Performance below 70 dB SPL is determined primarily by the HSR and MSR fibers, while the LSR fibers determine performance above 90 dB SPL.

Predictions based on the populations of coincidence counters are shown in the bottom row of Fig. 9 and are compared to human performance measured by Florentine *et al.* (1987) as a function of sensation level for the same low- and high-frequency tone conditions.[2] Human performance measured by Viemeister (1983) for level discrimination of a high-frequency, narrow-band noise in quiet is shown for comparison in the bottom right panel. At low frequencies, performance based on the HSR population is always better than performance based on the MSR and LSR populations, similar to the all-information predictions. Above 90 dB SPL, all three SR groups contribute essentially equally. Overall performance based on the total population of coincidence counters is more than an order of magnitude worse than optimal performance, but matches human performance very closely. Predicted performance is slightly better (within a factor of 2) than human performance at most levels. The slope of the near-miss to Weber's law observed in the human performance is matched by the coincidence predictions for the low-frequency tone, as well as by the near-miss beginning at 30 dB SPL. The near-miss in the coincidence predictions results primarily from the nonlinear-phase cues (which begin at 30 dB SPL) in the HSR fibers, and it is not influenced by the population of LSR fibers.

At high frequencies (Fig. 9, bottom right panel), coincidence performance based on the HSR fibers is best among the three SR groups below 80 dB SPL. Coincidence performance based on the total AN population matches the human performance very closely and is within a factor of 2 of both data sets at all levels. The nonmonotonic dependence on level (the "mid-level bump") observed in both sets of human data is also demonstrated in the coincidence predictions. The

level at which the bump occurs is well predicted by the coincidence performance. The size of the bump in the coincidence performance matches the data from Viemeister (1983) and is slightly smaller than the data from Florentine *et al.* (1987). A slight rise in ΔL as level increases at high levels is present in the coincidence performance and is predicted based on the spread of the high-frequency information beyond the highest CF in the model. A slight rise is also often observed in human data when plotted as a function of SPL (Florentine *et al.*, 1987).

IV. DISCUSSION

It has often been suggested that the cochlear amplifier is responsible for the extremely wide dynamic range of the auditory system (e.g., Yates, 1995). However, this suggestion has typically been based solely on the compressive magnitude response observed on the basilar membrane. The present study quantifies the information available for level discrimination in the auditory nerve (AN) with and without the nonlinear gain and nonlinear phase responses that are associated with the cochlear amplifier.

A. The benefit of the cochlear amplifier for extending the dynamic range within narrow CF regions

The encoding of sound level within narrow CF regions has been studied psychophysically using notched-noise maskers; however, understanding mechanisms by which stimulus level within restricted CF regions can be robustly encoded has important implications for wide-band stimuli (such as speech), which often have independent information in many frequency regions.

1. Nonlinear gain

The ability of humans to discriminate changes in level consistently across a wide range of levels in Viemeister's (1983) notched-noise experiment has been interpreted as demonstrating that Weber's law is achieved based on average rate within a narrow range of CFs (e.g., Delgutte, 1987). The notched-noise masker is presumed to mask the CFs away from the signal, and the high-frequency signal is presumed to rule out temporal information. The present predictions support this idea at high frequencies, where the amount of cochlear compression is large enough that the LSR fibers can encode changes in sound level at high levels (Fig. 7). Figure 6 demonstrates that the ability of LSR fibers to encode changes in high sound levels is due to the nonlinear (level-dependent) gain (i.e., compression) associated with the cochlear amplifier. Changes in level of the high-frequency tone were only encoded up to 70 dB SPL in the LSR fibers when the nonlinear gain response was removed from the AN model, but were encoded up to 100 dB SPL with the nonlinear gain.

At low frequencies, however, the average-rate information in a narrow CF region was not adequate to account for Weber's law. There was not enough cochlear compression at low frequencies to encode changes in level across the entire human dynamic range in the average rate of any of the three SR groups (Fig. 7). The model LSR fibers, which have a sloping saturation, only encode changes in level of the low-frequency tone up to 90 dB SPL based on average rate, and performance degrades significantly above 50 dB SPL. This result is consistent with predictions of level-discrimination performance based on cat AN fibers, for which ''straight'' rate-level curves are not observed (e.g., Sachs and Abbas, 1974; Delgutte, 1987; Viemeister, 1988a, 1988b; Winslow and Sachs, 1988). In contrast, Winter and Palmer (1991) predicted that level-discrimination performance for a 1-kHz tone based on guinea-pig AN fibers that innervate a single IHC was better than human performance up to at least 110 dB SPL; however, their model used compression values that were primarily determined from high-frequency fibers, and thus their model may not account for the reduced cochlear compression at low frequencies. Thus, while LSR fibers have been implicated in the encoding of sound level at high levels, they do not appear to quantitatively solve the dynamic-range problem at low frequencies.

2. Nonlinear phase

The nonlinear phase responses associated with the cochlear amplifier have rarely been considered for their ability to extend the dynamic range of the auditory system (Carney, 1994); however, they are significant because the wide dynamic range of their information about changes in level is present in all AN fibers, including the HSR fibers that comprise the majority of the AN population. Such a representation of level is preferred to the level-dependent combination schemes across SR groups that are required for average-rate information to account for level discrimination across a wide range of levels (Delgutte, 1987; Winslow *et al.*, 1987; Viemeister, 1988a, 1988b). For example, Winslow *et al.* (1987) have suggested that level could be encoded based on average rate with a level-dependent selective processor that relies on HSR fibers at low sound levels and LSR fibers at high levels (see review by May *et al.*, 1997). Figure 7 demonstrates that the nonlinear phase responses within a narrow range of CFs support Weber's law at low frequencies based on a combination of the three SR groups that is anatomically realistic (Liberman, 1978). In fact, performance based on the near-CF HSR fibers alone is relatively flat across the entire range of human hearing.

Carney (1994) has illustrated schematically how nonlinear phase shifts on single AN fibers produce systematic temporal patterns across CF (i.e., spatio-temporal patterns). She showed responses for a bank of model AN fibers with different CFs as a function of time for several stimulus levels (Fig. 5 Carney, 1994). The main feature of the spatio-temporal patterns is that, as level increases, the trajectory across CF of the peaks in the discharge probability as a function of time becomes steeper (i.e., the responses across CF become more coincident). This motivated her to propose that sound level may be encoded in the spatio-temporal discharge patterns of AN fibers, and that an across-frequency coincidence mechanism could utilize these level cues at medium to high levels. Figure 7 demonstrates quantitatively that a set of monaural, cross-frequency coincidence counters can encode sound level robustly across the entire range of human hearing based on AN fibers within a narrow range of CFs for both low- and high-frequency tones.

Because the cochlear amplifier acts primarily in near-CF regions, the benefits from both gain and phase cues for extending the dynamic range within narrow-CF regions are particularly useful for complex stimuli such as speech, where spread of excitation is limited. This suggestion is consistent with the general finding that hearing-impaired listeners have the most difficulty with complex stimuli in difficult listening conditions where spread of excitation may not be possible (Moore, 1995). Due to the rolloff in AN phase-locking above 2–3 kHz, the greatest benefit from nonlinear-phase cues is at low frequencies; however, the majority of important speech information is at low frequencies. The ability of nonlinear-phase information to account for Weber's law in narrow-CF regions at low frequencies (and the inability of average-rate information to do so), suggests that nonlinear-phase cues should be considered in the encoding of complex stimuli at high stimulus levels. Loss of the cochlear amplifier would be expected to degrade the representation of complex stimuli in impaired ears due to loss of the nonlinear-phase cues; however, this impairment would not be observed in physiological studies that quantify the reduction of AN information in impaired animals based only on average-rate and synchronized-rate responses (e.g., Miller *et al.*, 1997, 1999). In contrast, analyses of rate representations in the cochlear nucleus would be expected to demonstrate an impairment in the encoding of complex stimuli at high stimulus levels in impaired animals. The ability of monaural coincidence counters to encode changes in sound level at low frequencies across a much wider dynamic range than average-rate information in the AN may provide a basis for reports of enhanced rate representations in the cochlear nucleus. Blackburn and Sachs (1990) and May *et al.* (1998) have reported that rate representations of speech sounds are enhanced in the ventral cochlear nucleus (e.g., chopper neurons and primary-like units with low SR) compared with the AN in normal-hearing animals (reviewed by May *et al.*, 1997). Transient-chopper and primary-like-with-notch neurons in the cochlear nucleus have been shown to be sensitive to phase transitions across frequency, consistent with coincidence detection (Carney, 1990).

B. Pure-tone level discrimination in quiet

1. Near-miss to Weber's law at low frequencies

The present predictions suggest that the only effect of the nonlinear responses associated with the cochlear amplifier for level discrimination of low-frequency tones is that the near-miss, rather than Weber's law, is predicted based on the nonlinear phase responses. The degree of the near-miss in the all-information predictions is larger than in the rate-place predictions, but only matches human performance in the coincidence-detection predictions. Although there are many intuitive reasons to believe that cochlear nonlinearity would strongly influence level discrimination of tones, the predicted effect for tones in quiet is quite small. This nonintuitive finding results from the fact that at medium to high sound levels, where cochlear compression has a strong effect on near-CF BM responses, the primary information about changes in level is contributed by HSR fibers with CFs away from the frequency of the tone. Thus, the CFs that are dominating performance at medium and high sound levels are responding linearly because the nonlinear effects associated with the cochlear amplifier are restricted to near-CF frequencies.

Several other physiological models have produced a near-miss with only low-threshold, HSR fibers. Teich and Lachs (1979) demonstrated the near-miss with a rate-place model that had more rounded filter shapes than Siebert's filters and that incorporated the effects of refractoriness on AN discharge-count variance. Delgutte's (1987) model included average tuning-curve shaped filters and realistic AN-count variance. Heinz *et al.* (2001a) predicted a significant near-miss based on a computational AN model with linear gamma-tone filters and Poisson discharge statistics. The ability of many models to predict the near-miss based on different mechanisms supports the idea suggested by Viemeister (1988a) that the near-miss to Weber's law is not a critical aspect of the dynamic-range problem, and that the robust encoding of sound level in narrow-CF regions is the most important issue.

2. Mid-level bump at high frequencies

A puzzling detail of human level discrimination of tones in quiet is that performance is nonmonotonic at high frequencies, in contrast to the consistent improvement in performance with level at low frequencies (e.g., Carlyon and Moore, 1984; Florentine *et al.*, 1987). Many of the psychophysical experiments exploring the ''mid-level bump'' (or the ''severe departure from Weber's law'') have used short-duration signals in various noise maskers, because the effect (when reported as $\Delta I/I$) is generally larger for short-duration signals (e.g., Carlyon and Moore, 1984) and can be enhanced or reduced by various configurations of notched-noise maskers (e.g., Oxenham and Moore, 1995; Plack, 1998). However, the analytical AN model used in the present study is only appropriate to compare to long duration conditions because onset/offset responses and neural adaptation are not included in the model. In addition, the effects of a notched-noise masker on the different types of AN information must be considered quantitatively using methods that are beyond the present study, as discussed below. Thus, the high-frequency mid-level bump reported by Florentine *et al.* (1987) for level discrimination of 500-ms pure tones in quiet is an appropriate comparison for the present predictions.

Plack (1998) has discussed several explanations for the mid-level bump based on both peripheral and central mechanisms; however, only those that are addressed by the present predictions are discussed here. Carlyon and Moore (1984) have suggested that the mid-level bump at high frequencies may be explained by two populations of AN fibers. They suggested that good performance was provided by the low-threshold, HSR fibers at low levels and by the high-threshold, LSR fibers at high levels, with a degradation in performance at mid levels because neither population encoded changes in sound level. The absence of the mid-level bump at low frequencies was suggested to result from synchrony information providing good performance at mid-levels. The present predictions do not support this explanation by Carlyon and Moore (1984). For the high-frequency

tone, the transition between HSR and LSR fibers determining performance occurs near 80–90 dB SPL (Fig. 9), and no degradation in performance occurs because of the contribution of the third SR group (MSR) reported by Liberman (1978). The contribution of synchrony information at low frequencies is restricted to levels below those where HSR fibers contribute rate information (Fig. 9), and thus cannot be responsible for good performance at mid-levels. It was suggested by von Klitzing and Kohlrausch (1994) that the mid-level bump can be explained based on mid-level compression on the BM; however, their explanation requires that BM responses become linear above roughly 50 dB SPL, which has been shown not to be true in healthy cochleae (Ruggero *et al.*, 1997).

The present predictions demonstrate that a mid-level bump that is consistent with human data results from the large amount of cochlear compression at high frequencies (Figs. 8 and 9). The degradation in model performance at mid-levels is due to the BM input–output function becoming strongly compressed at 30 dB SPL (Fig. 8). As level increases further, the spread of excitation goes beyond the near-CF nonlinear region, and performance is dominated by HSR AN fibers that are responding linearly. Thus, the nonlinear-AN-model predictions for the HSR fibers match those from the linear AN model at levels above 60 dB SPL. The lack of a mid-level bump at low frequencies in the model predictions is consistent with the small amount of cochlear compression at low frequencies [Fig. 1(c)].

Thus, the present predictions suggest that the main effect of compressive magnitude responses on level discrimination of high-frequency tones in quiet is a degradation in performance at mid levels. This hypothesis suggests that hearing-impaired listeners without a healthy cochlear amplifier would not show a mid-level bump. However, this would be difficult to measure due to the typically limited dynamic range in hearing-impaired listeners (Florentine *et al.*, 1993).

In general, the effect of cochlear nonlinearity on level discrimination of tones in quiet was predicted to be small, because the influence of the cochlear amplifier is restricted to near-CF frequencies and the role of spread of excitation is large for tones in quiet. This small predicted effect is consistent with hearing-impaired listeners showing normal JNDs at equal SPL for suprathreshold conditions (Florentine *et al.*, 1993; Schroder *et al.*, 1994).

C. Coincidence detection: A robust, physiologically realistic neural mechanism

The predictions from the present study suggest that a set of monaural, cross-frequency coincidence counters that receive AN inputs from a narrow range of CFs can account for Weber's law across the dynamic range of human hearing, both at low and high frequencies. This finding is significant because Weber's law in narrow-CF regions appears to be required to account for human level-discrimination performance (Florentine and Buus, 1981; Viemeister, 1983); however, an optimal combination of average-rate information across the set of three SR groups in the AN does not produce Weber's law across a wide range of levels, at least at low frequencies (Fig. 7; Colburn, 1981; Delgutte, 1987).

Coincidence detection is a physiologically realistic mechanism, because any neuron with multiple subthreshold inputs acts as a coincidence detector (i.e., several nearly coincident discharges across the inputs are required to produce an output discharge). There is strong evidence that coincidence detection occurs in the binaural auditory system (Yin and Chan, 1990; Goldberg and Brown, 1969; Rose *et al.*, 1966; Yin *et al.*, 1987; Joris *et al.*, 1998), and coincidence detection forms the basis of most models of binaural processing (Colburn, 1996). Carney (1990) showed that several low-CF cell types in the antero-ventral cochlear nucleus (AVCN), primarily globular bushy cells, were sensitive to changes in the relative phase across their inputs. Joris *et al.* (1994a, 1994b) have provided evidence for monaural coincidence detection at all CFs in similar AVCN cell types based on enhanced synchronization in low- and high-CF cells to low-frequency tones.

The simple coincidence-counting mechanism analyzed in the present analysis was shown to utilize the level-dependent phase cues associated with the cochlear amplifier, as suggested by Carney (1994). In addition, the present study demonstrates that monaural, cross-frequency coincidence detection is a robust mechanism for encoding sound level in that both average-rate and nonlinear-phase information from AN discharges are encoded in the coincidence counts, as well as some information from synchrony cues. Thus, coincidence detection may account for level discrimination of noise as well, by decoding average-rate increases at low noise levels and increases in across-CF correlation due to broadened tuning at high levels (see Carney, 1994).

Overall coincidence-based performance depends on the implementation of the coincidence counter population, which was chosen to be simple and conservative in the present study. Inclusion of every AN fiber as an input to the coincidence population allowed the efficiency of the coincidence mechanism to be evaluated. Allowing each AN fiber to innervate only one coincidence neuron created an independent population for which performance could be more easily calculated. This implementation provided a conservative estimate of coincidence-based performance because allowing AN fibers to innervate more than one coincidence neuron could only improve performance (as long as potential across-neuron correlation was accounted for in the combination across coincidence counts).

It is generally accepted that there is far more information in AN responses than is used by humans, and that an inefficient processor is needed to account for human level-discrimination performance (e.g., Colburn, 1981; Delgutte, 1987). The coincidence-counting model processes the AN discharge times inefficiently. Information is lost in the process of coincidence detection because only the times of coincident AN discharges are considered. Additional information is lost by basing performance only on the coincidence counts (i.e., by ignoring the coincidence times). Even though the coincidence mechanism in the present study is far from optimal, the coincidence-performance predictions are typically shifted upward roughly in parallel from the all-information predictions. Figures 7 and 9 illustrate that the degradation in performance that occurs due to the coinci-

dence mechanism results in absolute performance levels for level discrimination that are very close to human performance. In addition, the monaural coincidence mechanism eliminates the requirement of an inefficient processor that varies its inefficiency as a function of level, which has been suggested based on average-discharge rate information in the AN (Colburn, 1981; Delgutte, 1987).

The derivations of performance based on a monaural, cross-frequency coincidence counter described in Appendix B suggest an interesting property that could be useful for physiological studies of neurons that are hypothesized to perform coincidence detection. The ratio of the expected value of coincidence counts [Eq. (B12)] to the variance of counts [Eq. (B13)] is dependent only on the properties of the temporal coincidence window $f(x)$. This ratio would be expected to be independent of stimulus parameters, and therefore the statistics of the observed discharge counts may be used to make inferences about the shape and size of the coincidence window of a given neuron.

D. Limitations of the present study

The analytical AN model was kept simple for the purposes of the present study. The model does not include the effects of external- and middle-ear filtering, or onset/offset and adaptation responses. Also, the model does not include many complex AN response properties, including refractory behavior, the effects of the olivocochlear efferent system (Guinan, 1996), and several complex irregularities in response to high-level tones (e.g., Liberman and Kiang, 1984; Kiang, 1984, 1990; Ruggero *et al.*, 1996) and clicks (Lin and Guinan, 2000). The absence of these properties does not limit the basic conclusions of the present study, but does limit the applicability of the present model at high levels and for more complex stimuli, as discussed further in Heinz (2000).

Predictions in the present study were compared to human data for level discrimination in a notched noise based on the common assumption that the only effect of the notched noise is to eliminate spread of excitation of the tone. In order to accurately evaluate the validity of this assumption, the effect of the noise masker on different types of information must be quantified. This analysis requires two advances beyond the present study: (1) a more complex AN model and (2) an extension of the signal detection theory (SDT) analysis.

In order to accurately evaluate complex stimuli, the AN model must include a description of suppression properties (e.g., Sachs and Kiang, 1968; Delgutte, 1990; Ruggero *et al.*, 1992). The AN response to a CF tone in the presence of a notched-noise masker may be suppressed by the noise, whereas the response of AN fibers with CFs within the noise may be suppressed by the tone. Such complex interactions between the tone and noise maskers could contribute significant information to detection or discrimination of signals in noise and therefore need to be quantified.

For cases in which the stimulus is random, an extension of the SDT analysis beyond the present study is required to quantify the relative effects of physiological (internal) and stimulus (external) variation on psychophysical performance. Heinz *et al.* (2001b) have described an extension of the SDT analysis to discrimination tasks in which a single parameter is randomly varied (e.g., random level variation). In addition, a general theoretical analysis of detection or discrimination of a signal in random noise has been developed and applied to the detection of tones in notched noise by Heinz (2000).

V. CONCLUSIONS

The cochlear amplifier benefits normal-hearing listeners by extending the dynamic range within narrow frequency regions. Nonlinear phase responses near CF associated with the cochlear amplifier encode changes in level across the entire dynamic range of hearing at low frequencies; however, the rolloff in phase locking reduces the effectiveness of phase cues at high frequencies for simple stimuli. Highly compressive basilar-membrane responses at high frequencies allow for the robust encoding of level based on average discharge rate; however, the reduction in cochlear compression at low frequencies reduces the relative ability of average rate to robustly encode sound level at low frequencies.

Cochlear nonlinearity has only a small effect on suprathreshold level discrimination of pure tones in quiet because performance is dominated by spread of excitation to linear off-CF responses. The only effects of cochlear nonlinearity predicted by the model for this task are the ''near-miss'' to Weber's law at low frequencies and the nonmonotonic ''mid-level bump'' at high frequencies.

Monaural coincidence detection is a physiologically realistic mechanism that can utilize the nonlinear gain and phase cues provided by the cochlear amplifier. Performance based on a population of coincidence counters matches human performance for level discrimination of tones across the entire dynamic range of hearing at both low and high frequencies.

ACKNOWLEDGMENTS

The authors thank Dr. Torsten Dau, Dr. Bertrand Delgutte, and Susan Early for providing valuable comments on an earlier version of this paper. We thank Dr. Don Johnson for his synchrony data from cat shown in Fig. 1(e), and Dr. Mario Ruggero for providing the data shown in Fig. 1(g). This study was part of a graduate dissertation in the Speech and Hearing Sciences Program of the Harvard–MIT Division of Health Sciences and Technology (Heinz, 2000). This work was supported in part by the National Institute of Health, Grant T32DC00038, and by the National Science Foundation, Grant 9983567.

APPENDIX A: NONLINEAR ANALYTICAL AUDITORY-NERVE MODEL

The analytical nonlinear auditory-nerve (AN) model used in the present study includes simple descriptions of the most significant properties of the cochlear amplifier. This model was kept as simple as possible so that basic concepts related to rate and timing cues associated with the cochlear amplifier could be demonstrated without the difficulty of interpreting predictions from a more complex model. The as-

sumptions and equations that specify the analytical model are described in this appendix, and basic response properties are shown in Fig. 1.

The discharge statistics of AN fibers are assumed to be described by a nonstationary Poisson process with a time-varying rate function $r(t)$. Equation (1) describes the phase-locked response of an AN fiber in response to a tone burst. The average discharge rate $\bar{r}[L_{\text{eff}}]$ and the strength of phase locking $g[L_{\text{eff}}, f_0]$ both depend on the effective level L_{eff} that drives each AN fiber.

The effective level for the ith AN fiber is determined by the tone level L (dB SPL) and by the nonlinear-filter magnitude response $H_{\text{NL}}(f_0, \text{CF}_i, L)$ for the characteristic frequency CF_i and the tone frequency f_0, i.e.,

$$L_{\text{eff}}(L, f_0, \text{CF}_i) = L + 20\log_{10}[H_{\text{NL}}(f_0, \text{CF}_i, L)]. \tag{A1}$$

The implementation of nonlinear tuning in the present model [see Figs. 1(a)–(c)] represents the idea that the cochlear amplifier produces high sensitivity and sharp tuning at low levels by providing amplification to near-CF frequencies, and that the cochlear-amplifier gain is reduced as level increases (Yates, 1995). At low levels, the magnitude response is described by linear triangular filters that are consistent with those used by Siebert (1968, 1970) to describe tuning curves in cat [see Fig. 1(a)], i.e.,

$$H_S\left(\frac{f_0}{\text{CF}_i}\right) = \begin{cases} \left(\dfrac{f_0}{\text{CF}_i}\right)^{10}, & f_0 \leqslant \text{CF}_i; \\ \left(\dfrac{f_0}{\text{CF}_i}\right)^{-20}, & f_0 \geqslant \text{CF}_i. \end{cases} \tag{A2}$$

Nonlinear compression is incorporated into the magnitude response H_{NL} by multiplying the linear triangular magnitude response H_S by a level- and frequency-dependent attenuation factor, i.e.,

$$H_{\text{NL}}(f_0, \text{CF}_i, L) = (10^{\gamma_{\text{dB}}(f_0, \text{CF}_i, L)/20}) H_S\left(\frac{f_0}{\text{CF}_i}\right). \tag{A3}$$

This form is used so that the level- and frequency-dependent attenuation $\gamma_{\text{dB}}(f_0, \text{CF}_i, L)$ is specified in dB, which allows model properties to be matched directly to experimental descriptions of responses associated with the cochlear amplifier. The next few expressions describe the frequency and level dependence of this attenuation.

The reduction in gain of the cochlear amplifier, γ_{dB}, is specified based on several simple assumptions, consistent with physiological findings (e.g., Ruggero *et al.*, 1997): (1) For a given CF, the maximum gain G provided by the cochlear amplifier is produced for tones presented at CF, and G in dB increases with CF [see Fig. 1(c)] according to

$$G(\text{CF}_i) = \begin{cases} G_{\min}, & \text{CF}_i \leqslant 500\ \text{Hz}; \\ G_{\min} + (G_{\max} - G_{\min}) \dfrac{\log_{10}(\text{CF}_i/500)}{\log_{10}(8000/500)}, & \\ \qquad 500 \leqslant \text{CF}_i \leqslant 8000\ \text{Hz}; & \\ G_{\max}, & \text{CF}_i \geqslant 8000\ \text{Hz}; \end{cases} \tag{A4}$$

where $G_{\min} = 20$ dB, $G_{\max} = 60$ dB. (2) The cochlear amplifier provides full gain for levels below $L_{\text{thr}}^{\text{NL}} = 30$ dB SPL, and the cochlear-amplifier gain is systematically reduced as level increases from $L_{\text{thr}}^{\text{NL}}$ to $L_{\text{sat}}^{\text{NL}} = 120$ dB SPL [see Fig. 1(b)]. (3) The cochlear amplifier only provides amplification for stimulus frequencies near CF, i.e., $f_{lf}^{\text{NL}} \leqslant f_0 \leqslant f_{hf}^{\text{NL}}$, where

$$\begin{aligned} f_{lf}^{\text{NL}} &= \text{CF}_i[10^{-G_{\max}/(20\cdot 10)}], \\ f_{hf}^{\text{NL}} &= \text{CF}_i[10^{G_{\max}/(20\cdot 20)}], \end{aligned} \tag{A5}$$

as shown in Fig. 1(a). This simple implementation of the nonlinear frequency region results in a flat magnitude response between f_{lf}^{NL} and f_{hf}^{NL} at high levels ($L \geqslant L_{\text{sat}}^{\text{NL}}$) and high characteristic frequencies ($\text{CF}_i \geqslant 8000$ Hz). Based on these assumptions, the level- and frequency-dependent reduction in gain is given in dB by

$$\begin{aligned} &\gamma_{\text{dB}}(f_0, \text{CF}_i, L) \\ &\quad = \beta_{\text{mag}}(L, f_0)\left\{-20\log_{10}\left[H_S\left(\frac{f_0}{\text{CF}_i}\right)\right] - G_{\max}\right\}\left[\frac{G(CF_i)}{G_{\max}}\right], \end{aligned} \tag{A6}$$

where

$$\beta_{\text{mag}}(L, f_0) = \begin{cases} 0, & L \leqslant L_{\text{thr}}^{\text{NL}} \quad \text{or} \quad f_0 \notin [f_{lf}^{\text{NL}}, f_{hf}^{\text{NL}}]; \\ \left(\dfrac{L - L_{\text{thr}}^{\text{NL}}}{L_{\text{sat}}^{\text{NL}} - L_{\text{thr}}^{\text{NL}}}\right), & \\ \qquad L_{\text{thr}}^{\text{NL}} \leqslant L \leqslant L_{\text{sat}}^{\text{NL}} \ \text{and} \ f_{lf}^{\text{NL}} \leqslant f_0 \leqslant f_{hf}^{\text{NL}}; & \\ 1, & L \geqslant L_{\text{sat}}^{\text{NL}} \ \text{and} \ f_{lf}^{\text{NL}} \leqslant f_0 \leqslant f_{hf}^{\text{NL}}. \end{cases} \tag{A7}$$

The parameter $\beta_{\text{mag}}(L, f_0)$ is a linear interpolation between the compression threshold $L_{\text{thr}}^{\text{NL}}$ and saturation level $L_{\text{sat}}^{\text{NL}}$ [see Fig. 1(b)], and it represents the reduction in cochlear-amplifier gain as level increases for near-CF frequencies. The second term in Eq. (A6) (in curly brackets) produces maximum gain at CF and reduced gain for tone frequencies off CF, and the third term controls the amount of gain as a function of CF.

In order to evaluate the effect of the nonlinear magnitude response on predictions in the present study, versions of the AN model with and without the nonlinear magnitude responses can be compared. The nonlinear magnitude responses can be excluded by setting $\beta_{\text{mag}}(L, f_0) = 0$ for all levels and frequencies.

The dependence of average discharge rate $\bar{r}$ on the effective level L_{eff} of an AN fiber is specified in terms of a simple saturating nonlinearity (based on Colburn, 1981)

$$\bar{r}[L_{\text{eff}}] = \begin{cases} \text{SR}, & L_{\text{eff}} \leqslant L_{\text{thr}} - 5; \\ \text{SR} + (1/600)(R_{\text{sat}} - \text{SR})(L_{\text{eff}} - L_{\text{thr}} + 5)^2, & \\ \qquad L_{\text{thr}} - 5 \leqslant L_{\text{eff}} \leqslant L_{\text{thr}} + 5; & \\ \text{SR} + (1/30)(R_{\text{sat}} - \text{SR})(L_{\text{eff}} - L_{\text{thr}}), & \\ \qquad L_{\text{thr}} + 5 \leqslant L_{\text{eff}} \leqslant L_{\text{thr}} + 30; & \\ R_{\text{sat}}, & L_{\text{eff}} \geqslant L_{\text{thr}} + 30; \end{cases} \tag{A8}$$

which depends on the spontaneous rate (SR), the saturated rate (R_{sat}), and the rate threshold (L_{thr}). The dependence of average rate on tone level L is shown for a high CF (maximum gain) and a low CF (small gain) in Figs. 1(d) and (f), respectively, for the three SR groups used in this study.

The dependence of phase locking on effective level L_{eff} is specified using the same general form of saturating nonlinearity, i.e.,

$$g[L_{\text{eff}},f_0]=\begin{cases}0, & L_{\text{eff}}\leqslant L_{\text{thr}}-25;\\ [g_{\max}(f_0)/600]\,(L_{\text{eff}}-L_{\text{thr}}+25)^2, & L_{\text{thr}}-25\leqslant L_{\text{eff}}\leqslant L_{\text{thr}}-15;\\ [g_{\max}(f_0)/30]\,(L_{\text{eff}}-L_{\text{thr}}+20), & L_{\text{thr}}-15\leqslant L_{\text{eff}}\leqslant L_{\text{thr}}+10;\\ g_{\max}(f_0), & L_{\text{eff}}\geqslant L_{\text{thr}}+10;\end{cases} \tag{A9}$$

where the dependence of synchrony on frequency, $g_{\max}(f_0)$, is matched to data from cat [see Fig. 1(e); Johnson, 1980], and is described by

$$g_{\max}(f_0)=\begin{cases}3.1, & f_0\leqslant 1200\ \text{Hz};\\ \dfrac{3.1*1200}{f_0}, & 1200\leqslant f_0\leqslant 2800\ \text{Hz};\\ \dfrac{3.1*1200*2800^2}{(f_0)^3}, & f_0\geqslant 2800\ \text{Hz}.\end{cases} \tag{A10}$$

Note that the threshold for phase locking is specified to be 20 dB below the average-rate threshold in Eq. (A9).

The implementation of the nonlinear phase responses in the present study [see Fig. 1(h)] is based on several simple assumptions: (1) The level-dependent phase responses are limited to the same near-CF frequency region as the magnitude responses, $f_{lf}^{\text{NL}}\leqslant f_0\leqslant f_{hf}^{\text{NL}}$. (2) Phase varies linearly with tone level. (3) The maximum phase changes occur half way into the near-CF nonlinear frequency region, i.e., at frequencies

$$f_{lf}^{\text{PH}}=0.5(\text{CF}_i+f_{lf}^{\text{NL}}),\quad f_{hf}^{\text{PH}}=0.5(\text{CF}_i+f_{hf}^{\text{NL}}). \tag{A11}$$

(4) The maximum phase shifts between low levels and 80 dB SPL are roughly $\pi/2$. (5) The total traveling-wave delay at high levels ($L>L_{\text{sat}}^{\text{NL}}$) is compensated for in each CF with neural delays prior to innervation of the coincidence-detection population. This simple assumption is based on strong onset responses to tones for many cell types in the cochlear nucleus (Young, 1984; Rhode and Greenberg, 1992). Based on these simple assumptions, the compensated nonlinear filter phase response [see Fig. 1(h)] is specified by the equation

$$\theta(f_0,\text{CF}_i,L)=\begin{cases}0, & f_0\notin[f_{lf}^{\text{NL}},f_{hf}^{\text{NL}}];\\ \beta_{\text{phase}}(L,f_0)\cdot 2\Delta\theta_{\max}\left(\dfrac{f_0-f_{lf}^{\text{NL}}}{\text{CF}_i-f_{lf}^{\text{NL}}}\right), & f_{lf}^{\text{NL}}\leqslant f_0\leqslant f_{lf}^{\text{PH}};\\ \beta_{\text{phase}}(L,f_0)\cdot 2\Delta\theta_{\max}\left(\dfrac{\text{CF}_i-f_0}{\text{CF}_i-f_{lf}^{\text{NL}}}\right), & f_{lf}^{\text{PH}}\leqslant f_0\leqslant \text{CF}_i;\\ \beta_{\text{phase}}(L,f_0)\cdot 2\Delta\theta_{\max}\left(\dfrac{\text{CF}_i-f_0}{f_{hf}^{\text{NL}}-\text{CF}_i}\right), & \text{CF}_i\leqslant f_0\leqslant f_{hf}^{\text{PH}};\\ \beta_{\text{phase}}(L,f_0)\cdot 2\Delta\theta_{\max}\left(\dfrac{f_0-f_{hf}^{\text{NL}}}{f_{hf}^{\text{NL}}-\text{CF}_i}\right), & f_{hf}^{\text{PH}}\leqslant f_0\leqslant f_{hf}^{\text{NL}};\end{cases} \tag{A12}$$

where $\Delta\theta_{\max}=\frac{6}{5}\pi$ is the maximum phase change between $L_{\text{thr}}^{\text{NL}}$ and $L_{\text{sat}}^{\text{NL}}$, and $\beta_{\text{phase}}(L,f_0)=1-\beta_{\text{mag}}(L,f_0)$, where $\beta_{\text{mag}}(L,f_0)$ is specified by Eq. (A7).

Versions of the AN model with and without the nonlinear phase changes can be compared in order to evaluate the effect of nonlinear phase responses. The level-dependent phase changes can be excluded by setting $\beta_{\text{phase}}(L,f_0)=1$ for all levels and frequencies.

APPENDIX B: PERFORMANCE BASED ON A MONAURAL COINCIDENCE COUNTER

This appendix presents derivations of the expected value and variance of the coincidence counts $\mathcal{C}_{ij}\{\mathcal{T}^i,\mathcal{T}^j\}$ [Eq. (2)] that are needed to calculate the normalized sensitivity δ' of a monaural, cross-frequency coincidence counter [Eq. (6)]. Similar equations and related discussions are presented without derivations by Colburn (1969, 1977b) for a binaural coincidence counter. The expected value and variance in Eq. (6) depend on the Poisson statistics of the two sets of independent AN discharge times, $\mathcal{T}^i$ and $\mathcal{T}^j$, and will be shown to be given by

$$E_{\mathcal{T}^i,\mathcal{T}^j,\phi}[\mathcal{C}_{ij}\{\mathcal{T}^i,\mathcal{T}^j\}]=E_\phi\left[\int_0^T\int_0^T f(x-y)r_i(x;\phi)r_j(y;\phi)\,dx\,dy\right], \tag{B1}$$

$$\text{Var}_{\mathcal{T}^i,\mathcal{T}^j,\phi}[\mathcal{C}_{ij}\{\mathcal{T}^i,\mathcal{T}^j\}]\simeq E_\phi\left[\int_0^T\int_0^T f^2(x-y)r_i(x;\phi)r_j(y;\phi)\,dx\,dy\right], \tag{B2}$$

where $r_i(t;\phi)$ and $r_j(t;\phi)$ represent the time-varying rate functions of the two AN inputs to the coincidence counter, ϕ is a random phase imposed on every AN fiber (to force the lack of an absolute time or phase reference), and $f(x)$ is the narrow temporal coincidence window.

The derivations of Eqs. (B1) and (B2) rely on several general results for decision variables of the form

$$X_i(\mathcal{T}^i)=\sum_{l=1}^{K_i}s(t_l^i), \tag{B3}$$

where $s(t_l^i)$ is any function of the lth discharge time t_l^i generated from a Poisson process with rate function $r_i(t)$. It can

be shown (e.g., Rieke *et al.*, 1997) that the expected value and variance of $X_i(\mathcal{T}^i)$ are given by

$$E_{\mathcal{T}^i}[X_i(\mathcal{T}^i)] = \int_0^T s(t) r_i(t)\, dt, \tag{B4}$$

$$\mathrm{Var}_{\mathcal{T}^i}[X_i(\mathcal{T}^i)] = \int_0^T s^2(t) r_i(t)\, dt, \tag{B5}$$

based on the probability density function for Poisson discharge times (see Parzen, 1962; Snyder and Miller, 1991). Equations (B4) and (B5) imply that

$$E_{\mathcal{T}^i}\{[X_i(\mathcal{T}^i)]^2\} = \int_0^T s^2(t) r_i(t)\, dt + \left[\int_0^T s(t) r_i(t)\, dt\right]^2. \tag{B6}$$

The expected value of the coincidence counts [used in Eq. (6) of the text] can be derived as follows:

$$\begin{aligned} E_{\mathcal{T}^i,\mathcal{T}^j,\phi}[\mathcal{C}_{ij}\{\mathcal{T}^i,\mathcal{T}^j\}] &= E_{\mathcal{T}^i,\mathcal{T}^j,\phi}\left[\sum_{l=1}^{K_i}\sum_{m=1}^{K_j} f(t_l^i - t_m^j)\right] \\ &= E_{\mathcal{T}^i,\phi}\left\{\sum_{l=1}^{K_i} E_{\mathcal{T}^j}\left[\sum_{m=1}^{K_j} f(t_l^i - t_m^j)\,\middle|\, \mathcal{T}^i\right]\right\} \\ &= E_{\mathcal{T}^i,\phi}\left[\sum_{l=1}^{K_i}\int_0^T f(t_l^i - y) r_j(y;\phi)\, dy\right]. \end{aligned} \tag{B7}$$

Using Eq. (B4) again, Eq. (B1) is obtained. Similarly, the term $E_{\mathcal{T}^i,\mathcal{T}^j,\phi}[\mathcal{C}_{ij}^2\{\mathcal{T}^i,\mathcal{T}^j\}]$ can be derived as follows:

$$\begin{aligned} &E_{\mathcal{T}^i,\mathcal{T}^j,\phi}[\mathcal{C}_{ij}^2\{\mathcal{T}^i,\mathcal{T}^j\}] \\ &= E_{\mathcal{T}^i,\phi}\left[E_{\mathcal{T}^j}\left(\left\{\sum_{m=1}^{K_j}\left[\sum_{l=1}^{K_i} f(t_l^i - t_m^j)\right]\right\}^2 \middle| \mathcal{T}^i\right)\right] \\ &= E_{\mathcal{T}^i,\phi}\left\{\int_0^T\left[\sum_{l=1}^{K_i} f(t_l^i - y)\right]^2 r_j(y;\phi)\, dy + \left[\sum_{l=1}^{K_i}\int_0^T f(t_l^i - y) r_j(y;\phi)\, dy\right]^2\right\} \\ &= E_\phi\left\{\int_0^T\int_0^T f^2(x-y) r_i(x;\phi) r_j(y;\phi)\, dx\, dy + \int_0^T\int_0^T\int_0^T f(x-y) f(u-y) r_i(x;\phi) r_i(u;\phi) r_j(y;\phi)\, dx\, du\, dy \right. \\ &\quad + \int_0^T\int_0^T\int_0^T f(x-y) f(x-v) r_i(x;\phi) r_j(v;\phi) r_j(y;\phi)\, dx\, dv\, dy + \left.\left[\int_0^T\int_0^T f(x-y) r_i(x;\phi) r_j(y;\phi)\, dx\, dy\right]^2\right\}. \end{aligned} \tag{B8}$$

The variance in Eq. (6) is then equal to

$$\begin{aligned} &\mathrm{Var}_{\mathcal{T}^i,\mathcal{T}^j,\phi}[\mathcal{C}_{ij}\{\mathcal{T}^i,\mathcal{T}^j\}] \\ &= E_{\mathcal{T}^i,\mathcal{T}^j,\phi}[\mathcal{C}_{ij}^2\{\mathcal{T}^i,\mathcal{T}^j\}] - (E_{\mathcal{T}^i,\mathcal{T}^j,\phi}[\mathcal{C}_{ij}\{\mathcal{T}^i,\mathcal{T}^j\}])^2 \\ &= E_\phi\left\{\int_0^T\int_0^T f^2(x-y) r_i(x;\phi) r_j(y;\phi)\, dx\, dy \right. \\ &\quad + \int_0^T\int_0^T\int_0^T f(x-y) f(u-y) r_i(x;\phi) r_i(u;\phi) r_j(y;\phi)\, dx\, du\, dy \\ &\quad + \left.\int_0^T\int_0^T\int_0^T f(x-y) f(x-v) r_i(x;\phi) r_j(v;\phi) r_j(y;\phi)\, dx\, dv\, dy\right\}. \end{aligned} \tag{B9}$$

The two triple-integral terms in the right-hand side of Eq. (B9) can be shown to be negligible relative to the double-integral term if (1) the coincidence window $f(x)$ is much narrower than the period of variation in discharge rate $r(t)$, which is never less than about 0.5 ms given the rolloff in phase locking of AN fibers above 2 kHz [Fig. 1(e); Johnson (1980)], and (2) the following inequality holds:

$$R_{\mathrm{sat}}\left[\int_{-\infty}^{\infty} f(x)\, dx\right]^2 \ll \int_{-\infty}^{\infty} f^2(x)\, dx, \tag{B10}$$

where R_{sat} is the maximum discharge rate of an AN fiber. Both of these conditions are satisfied for the 10-μs rectangular coincidence window in the present study, and thus the approximation in Eq. (B2) holds.

Note that Eqs. (B1) and (B2) can be used with either analytical or computational AN models because they are independent of the AN model used to produce the rate functions. More informative expressions for the expected value and variance can be derived for the present analytical AN model. The expected value can be derived by substituting the rate function $r(t)$ from the analytical AN model [Eq. (1)] into Eq. (B1), i.e.,

$$E_{\mathcal{T}^i,\mathcal{T}^j,\phi}[\mathcal{C}_{ij}\{\mathcal{T}^i,\mathcal{T}^j\}] = \frac{\overline{r_i r_j}}{I_0[g_i]I_0[g_j]} \int_0^T \int_0^T f(x-y)\frac{1}{2\pi}\int_0^{2\pi} \exp[g_i \cos(2\pi f_0 x+\theta_i+\phi)+g_j \cos(2\pi f_0 y+\theta_j+\phi)]\,d\phi\,dx\,dy$$

$$= \frac{\overline{r_i r_j}}{I_0[g_i]I_0[g_j]} \int_0^T \int_0^T f(x-y)\frac{1}{2\pi}\int_0^{2\pi} \exp\Bigg(\sqrt{g_i^2+g_j^2+2g_i g_j \cos[2\pi f_0(x-y)+\theta_i-\theta_j]}$$

$$\times \cos\Bigg\{ \phi + \tan^{-1}\Bigg[\frac{g_i \sin(2\pi f_0 x+\theta_i)+g_j \sin(2\pi f_0 y+\theta_j)}{g_i \cos(2\pi f_0 x+\theta_i)+g_j \cos(2\pi f_0 y+\theta_j)} \Bigg] \Bigg\} \Bigg) d\phi\,dx\,dy$$

$$= \frac{\overline{r_i r_j}}{I_0[g_i]I_0[g_j]} \int_0^T \int_0^T f(x-y) I_0\{\sqrt{g_i^2+g_j^2+2g_i g_j \cos[2\pi f_0(x-y)+\theta_i-\theta_j]}\}dx\,dy, \tag{B11}$$

where $g_i = g[L_{\text{eff}}(L,f_0,\text{CF}_i),f_0]$, $\overline{r_i} = \overline{r}[L_{\text{eff}}(L,f_0,\text{CF}_i)]$, and $\theta_i = \theta(L,f_0,\text{CF}_i)$, and $I_0\{g\}$ is the zeroth-order modified Bessel function of the first kind. The second form follows from writing the sum of cosines as a single cosine, and the last expression follows from the insensitivity of the integral over a period to the phase angle.

Using the assumption that the coincidence window $f(x)$ is narrow relative to the period of stimulus variation, the expected value [Eq. (B1)] and variance [Eq. (B2)] can be shown to be approximated by

$$E[\mathcal{C}_{ij}|L] \simeq \frac{T\overline{r_i r_j}}{I_0[g_i]I_0[g_j]} I_0[\sqrt{g_i^2+g_j^2+2g_i g_j \cos(\theta_i-\theta_j)}] \times \int_{-\infty}^{\infty} f(x)dx, \tag{B12}$$

$$\text{Var}[\mathcal{C}_{ij}|L] \simeq \frac{T\overline{r_i r_j}}{I_0[g_i]I_0[g_j]} I_0[\sqrt{g_i^2+g_j^2+2g_i g_j \cos(\theta_i-\theta_j)}] \times \int_{-\infty}^{\infty} f^2(x)dx. \tag{B13}$$

[1]Coincidence counters for which one input fell outside the model CF range (300–20 000 Hz) were evaluated by using the edge model CF as the input instead. This end effect was not significant for this study's results.

[2]The data from Florentine *et al.* (1987) are plotted as a function of sensation level (SL), which is the most appropriate comparison to the predictions from the analytical AN model that has a fixed threshold at 0 dB SPL. Some of the effects in the human data that occur at a particular sensation level are reduced when the data is averaged across listeners as a function of SPL, rather than SL.

Anderson, D.J., Rose, J.E., Hind, J.E., and Brugge, J.F. (**1971**). "Temporal position of discharges in single auditory nerve fibers within the cycle of a sinewave stimulus: Frequency and intensity effects," J. Acoust. Soc. Am. **49**, 1131–1139.

Blackburn, C.C., and Sachs, M.B. (**1990**). "The representations of the steady-state vowel sound /ε/ in the discharge patterns of cat anteroventral cochlear nucleus neurons," J. Neurophysiol. **63**, 1191–1212.

Braida, L.D., and Durlach, N.I. (**1988**). "Peripheral and central factors in intensity perception," in *Auditory Function: Neurobiological Bases of Hearing*, edited by G.M. Edelman, W.E. Gall, and W.M. Cowan (Wiley, New York), pp. 559–583.

Carlyon, R.P., and Moore, B.C.J. (**1984**). "Intensity discrimination: A severe departure from Weber's law," J. Acoust. Soc. Am. **76**, 1369–1376.

Carney, L.H. (**1990**). "Sensitivities of cells in the anteroventral cochlear nucleus of cat to spatiotemporal discharge patterns across primary afferents," J. Neurophysiol. **64**, 437–456.

Carney, L.H. (**1994**). "Spatiotemporal encoding of sound level: Models for normal encoding and recruitment of loudness," Hear. Res. **76**, 31–44.

Carney, L.H., Heinz, M.G., and Colburn, H.S. (**1999**). "Spatiotemporal coding of sound level: Quantifying the information provided by level-dependent phase cues," Abstracts of the 22nd Midwinter Meeting of the Association for Research in Otolaryngology, pp. 212–213.

Cheatham, M.A., and Dallos, P. (**1998**). "The level dependence of response phase: Observations from cochlear hair cells," J. Acoust. Soc. Am. **104**, 356–369.

Colburn, H.S. (**1969**). Ph.D. dissertation, Massachusetts Institute of Technology, Cambridge, MA.

Colburn, H.S. (**1973**). "Theory of binaural interaction based on auditory-nerve data. I. General strategy and preliminary results on interaural discrimination," J. Acoust. Soc. Am. **54**, 1458–1470.

Colburn, H.S. (**1977a**). "Theory of binaural interaction based on auditory-nerve data. II. Detection of tones in noise," J. Acoust. Soc. Am. **61**, 525–533.

Colburn, H.S. (**1977b**). "Theory of binaural interaction based on auditory-nerve data. II. Detection of tones in noise. Supplementary material," AIP Document No. PAPS JASMA-**61**-525-98.

Colburn, H.S. (**1981**). "Intensity perception: relation of intensity discrimination to auditory-nerve firing patterns," Internal Memorandum, Research Laboratory of Electronics, Massachusetts Institute of Technology, Cambridge, MA.

Colburn, H.S. (**1996**). "Computational models of binaural processing," in *Auditory Computation*, edited by H.L. Hawkins, T.A. McMullen, A.N. Popper, and R.R. Fay (Springer-Verlag, New York), pp. 332–400.

Cooper, N.P., and Rhode, W.S. (**1997**). "Mechanical responses to two-tone distortion products in the apical and basal turns of the mammalian cochlea," J. Neurophysiol. **78**, 261–270.

Dau, T., Püschel, D., and Kohlrausch, A. (**1996**). "A quantitative model of the 'effective' signal processing in the auditory system I. Model structure," J. Acoust. Soc. Am. **99**, 3615–3622.

Dau, T., Kollmeier, B., and Kohlrausch, A. (**1997**). "Modeling auditory processing of amplitude modulation. I. Detection and masking with narrow-band carriers," J. Acoust. Soc. Am. **102**, 2892–2905.

Delgutte, B. (**1987**). "Peripheral auditory processing of speech information: implications from a physiological study of intensity discrimination," in *The Psychophysics of Speech Perception*, edited by M.E.H. Schouten (Nijhoff, Dordrecht, The Netherlands), pp. 333–353.

Delgutte, B. (**1990**). "Two-tone rate suppression in auditory-nerve fibers: Dependence on suppressor frequency and level," Hear. Res. **49**, 225–246.

Delgutte, B. (**1996**). "Physiological models for basic auditory percepts," in *Auditory Computation*, edited by H.L. Hawkins, T.A. McMullen, A.N. Popper, and R.R. Fay (Springer-Verlag, New York), pp. 157–220.

Durlach, N.I., and Braida, L.D. (**1969**). "Intensity perception I: Preliminary theory of intensity resolution," J. Acoust. Soc. Am. **46**, 372–383.

Evans, E.F. (**1981**). "The dynamic range problem: Place and time coding at the level of cochlear nerve and nucleus," in *Neuronal Mechanisms of Hearing*, edited by J. Syka and L. Aitkin (Plenum, New York), pp. 69–85.

Fekete, D.M., Rouiller, E.M., Liberman, M.C., and Ryugo, D.K. (**1984**). "The central projections of intracellularly labeled auditory nerve fibers in cats," J. Comp. Neurol. **229**, 432–450.

Florentine, M., and Buus, S. (**1981**). "An excitation pattern model for intensity discrimination," J. Acoust. Soc. Am. **70**, 1646–1654.

Florentine, M., Buus, S., and Mason, C.R. (**1987**). "Level discrimination as a function of level for tones from 0.25 to 16 kHz," J. Acoust. Soc. Am. **81**, 1528–1541.

Florentine, M., Reed, C.M., Rabinowitz, W.M., Braida, L.D., Durlach, N.I., and Buus, S. (**1993**). ''Intensity perception. XIV. Intensity discrimination in listeners with sensorineural hearing loss,'' J. Acoust. Soc. Am. **94**, 2575–2586.

Geisler, C.D., and Rhode, W.S. (**1982**). ''The phases of basilar-membrane vibrations,'' J. Acoust. Soc. Am. **71**, 1201–1203.

Goldberg, J.M., and Brown, P.B. (**1969**). ''Response of binaural neurons of dog superior olivary complex to dichotic tonal stimuli: Some physiological mechanisms of sound localization,'' J. Neurophysiol. **32**, 613–636.

Green, D.M. and Swets, J.A. (**1966**). *Signal Detection Theory and Psychophysics* (Wiley, New York, reprinted 1988 by Peninsula, Los Altos, CA).

Greenwood, D.D. (**1990**). ''A cochlear frequency-position function for several species—29 years later,'' J. Acoust. Soc. Am. **87**, 2592–2605.

Gresham, L.C., and Collins, L.M. (**1998**). ''Analysis of the performance of a model-based optimal auditory signal processor,'' J. Acoust. Soc. Am. **103**, 2520–2529.

Guinan, J.J., Jr. (**1996**). ''Physiology of olivocochlear efferents,'' in *The Cochlea*, edited by P.J. Dallos, A.N. Popper, and R.R. Fay (Springer-Verlag, New York), pp. 435–502.

Heinz, M.G. (**2000**). Ph.D. dissertation, Massachusetts Institute of Technology, Cambridge, MA.

Heinz, M.G., Colburn, H.S., and Carney, L.H. (**2001a**). ''Evaluating auditory performance limits: I. One-parameter discrimination using a computational model for the auditory nerve,'' Neural Computation **13**, 2273–2316.

Heinz, M.G., Colburn, H.S., and Carney, L.H. (**2001b**). ''Evaluating auditory performance limits: II. One-parameter discrimination with random level variation,'' Neural Computation **13**, 2317–2339.

Hicks, M.L., and Bacon, S.P. (**1999**). ''Psychophysical measures of auditory nonlinearities as a function of frequency in individuals with normal hearing,'' J. Acoust. Soc. Am. **105**, 326–338.

Huettel, L.G., and Collins, L.M. (**1999**). ''Using computational auditory models to predict simultaneous masking data: Model comparison,'' IEEE Trans. Biomed. Eng. **46**, 1432–1440.

Jesteadt, W., Wier, C.C., and Green, D.M. (**1977**). ''Intensity discrimination as a function of frequency and sensation level,'' J. Acoust. Soc. Am. **61**, 169–177.

Johnson, D.H. (**1980**). ''The relationship between spike rate and synchrony in responses of auditory-nerve fibers to single tones,'' J. Acoust. Soc. Am. **68**, 1115–1122.

Johnson, D.H., and Kiang, N.Y.S. (**1976**). ''Analysis of discharges recorded simultaneously from pairs of auditory-nerve fibers,'' Biophys. J. **16**, 719–734.

Joris, P.X., Carney, L.H., Smith, P.H., and Yin, T.C.T. (**1994a**). ''Enhancement of neural synchronization in the anteroventral cochlear nucleus. I. Responses to tones at the characteristic frequency,'' J. Neurophysiol. **71**, 1022–1036.

Joris, P.X., Smith, P.H., and Yin, T.C.T. (**1994b**). ''Enhancement of neural synchronization in the anteroventral cochlear nucleus. II. Responses in the tuning curve tail,'' J. Neurophysiol. **71**, 1037–1051.

Joris, P.X., Smith, P.H., and Yin, T.C.T. (**1998**). ''Coincidence detection in the auditory system: 50 years after Jeffress,'' Neuron **21**, 1235–1238.

Kiang, N.Y.S. (**1984**). ''Peripheral neural processing of auditory information,'' in *Handbook of Physiology, Section I: The Nervous System, Vol. III, Pt. 2*, edited by J.M. Brookhart and V.B. Mountcastle (American Physiological Society, Bethesda, MD), pp. 639–674.

Kiang, N.Y.S. (**1990**). ''Curious oddments of auditory-nerve studies,'' Hear. Res. **49**, 1–16.

Kiang, N.Y.S., Watanabe, T., Thomas, E.C., and Clark, L.F. (**1965**). *Discharge Patterns of Single Fibers in the Cat's Auditory Nerve* (MIT Press, Cambridge, MA).

von Klitzing, R., and Kohlrausch, A. (**1994**). ''Effect of masker level on overshoot in running- and frozen-noise maskers,'' J. Acoust. Soc. Am. **95**, 2192–2201.

Liberman, M.C. (**1978**). ''Auditory-nerve response from cats raised in a low-noise chamber,'' J. Acoust. Soc. Am. **63**, 442–455.

Liberman, M.C. (**1991**). ''Central projection of auditory-nerve fibers of differing spontaneous rate. I. Anteroventral cochlear nucleus,'' J. Comp. Neurol. **313**, 240–258.

Liberman, M.C. (**1993**). ''Central projection of auditory-nerve fibers of differing spontaneous rate. II. Posteroventral and dorsal cochlear nuclei,'' J. Comp. Neurol. **327**, 17–36.

Liberman, M.C., and Kiang, N.Y.S. (**1984**). ''Single-neuron labeling and chronic cochlear pathology. IV. Stereocilia damage and alterations in rate- and phase-level functions,'' Hear. Res. **16**, 75–90.

Lin, T., and Guinan, J.J. Jr. (**2000**). ''Auditory-nerve-fiber responses to high-level clicks: Interference patterns indicate that excitation is due to the combination of multiple drives,'' J. Acoust. Soc. Am. **107**, 2615–2630.

May, B.J., and Sachs, M.B. (**1992**). ''Dynamic range of neural rate responses in the ventral cochlear nucleus of awake cats,'' J. Neurophysiol. **68**, 1589–1602.

May, B.J., Le Prell, G.S., Hienz, R.D., and Sachs, M.B. (**1997**). ''Speech representation in the auditory nerve and ventral cochlear nucleus: Quantitative comparisons,'' in *Acoustical Signal Processing in the Central Auditory System*, edited by J. Syka (Plenum, New York), pp. 413–429.

May, B.J., Le Prell, G.S., and Sachs, M.B. (**1998**). ''Vowel representations in the ventral cochlear nucleus of the cat: Effects of level, background noise, and behavioral state,'' J. Neurophysiol. **79**, 1755–1767.

McGill, W.J., and Goldberg, J.P. (**1968**). ''A study of the near-miss involving Weber's law and pure-tone intensity discrimination,'' Percept. Psychophys. **4**, 105–109.

Miller, M.I., Barta, P.E., and Sachs, M.B. (**1987**). ''Strategies for the representation of a tone in background noise in the temporal aspects of the discharge patterns of auditory-nerve fibers,'' J. Acoust. Soc. Am. **81**, 665–679.

Miller, R.L., Schilling, J.R., Franck, K.R., and Young, E.D. (**1997**). ''Effects of acoustic trauma on the representation of the vowel /ɛ/ in cat auditory nerve fibers,'' J. Acoust. Soc. Am. **101**, 3602–3616.

Miller, R.L., Calhoun, B.M., and Young, E.D. (**1999**). ''Discriminability of vowel representation in cat auditory nerve fibers after acoustic trauma,'' J. Acoust. Soc. Am. **105**, 311–325.

Moore, B.C.J. (**1995**). *Perceptual Consequences of Cochlear Damage* (Oxford University Press, New York).

Moore, B.C.J., and Oxenham, A.J. (**1998**). ''Psychoacoustic consequences of compression in the peripheral auditory system,'' Psychol. Rev. **105**, 108–124.

Nuttall, A.L., and Dolan, D.F. (**1996**). ''Steady-state sinusoidal velocity responses of the basilar membrane in guinea pig,'' J. Acoust. Soc. Am. **99**, 1556–1565.

Oxenham, A.J., and Moore, B.C.J. (**1995**). ''Overshoot and the ''severe departure'' from Weber's Law,'' J. Acoust. Soc. Am. **97**, 2442–2453.

Parzen, E. (**1962**). *Stochastic Processes* (Holden-Day, San Francisco), Chap. 4.

Patuzzi, R.B., Yates, G.K., and Johnstone, B.M. (**1989**). ''Outer hair receptor currents and sensorineural hearing loss,'' Hear. Res. **42**, 47–72.

Plack, C.J. (**1998**). ''Beneficial effects of notched noise on intensity discrimination in the region of the severe departure,'' J. Acoust. Soc. Am. **103**, 2530–2538.

Rabinowitz, W.M., Lim, J.S., Braida, L.D., and Durlach, N.I. (**1976**). ''Intensity perception VI: Summary of recent data on deviations from Weber's law for 1000-Hz tone pulses,'' J. Acoust. Soc. Am. **59**, 1506–1509.

Rasmussen, G.L. (**1940**). ''Studies of the VIIIth cranial nerve in man,'' Laryngoscope **50**, 67–83.

Rhode, W.S. (**1971**). ''Observations of the vibration of the basilar membrane in squirrel monkeys using the Mössbauer technique,'' J. Acoust. Soc. Am. **49**, 1218–1231.

Rhode, W.S., and Greenberg, S. (**1992**). ''Physiology of the cochlear nuclei,'' in *The Mammalian Auditory Pathway: Neurophysiology*, edited by A.N. Popper and R.R. Fay (Springer Verlag, New York), pp. 94–152.

Rieke, F., Warland, D., de Ruyter van Steveninck, R., and Bialek, W. (**1997**). *Spikes: Exploring the Neural Code* (MIT Press, Cambridge, MA).

Rose, J.E., Gross, N.B., Geisler, C.D., and Hind, J.E. (**1966**). ''Some neural mechanisms in the inferior colliculus of the cat which may be relevant to localization of a sound source,'' J. Neurophysiol. **29**, 288–314.

Rouiller, E.M., Cronin-Schreiber, R., Fekete, D.M., and Ryugo, D.K. (**1986**). ''The central projections of intracellularly labeled auditory nerve fibers in cats: an analysis of terminal morphology,'' J. Comp. Neurol. **249**, 261–278.

Ruggero, M.A. (**1992**). ''Physiology and coding of sound in the auditory nerve,'' in *The Mammalian Auditory Pathway: Neurophysiology*, edited by A.N. Popper and R.R. Fay (Springer-Verlag, New York), pp. 34–93.

Ruggero, M.A., Robles, L., and Rich, N.C. (**1992**). ''Two-tone suppression in the basilar membrane of the cochlea: Mechanical basis of auditory-nerve rate suppression,'' J. Neurophysiol. **68**, 1087–1099.

Ruggero, M.A., Rich, N.C., Shivapuja, B.G., and Temchin, A.N. (**1996**). ''Auditory-nerve responses to low-frequency tones: Intensity dependence,'' Aud. Neurosci. **2**, 159–185.

Ruggero, M.A., Rich, N.C., Recio, A., Narayan, S.S., and Robles, L. (**1997**). ''Basilar-membrane responses to tones at the base of the chinchilla cochlea,'' J. Acoust. Soc. Am. **101**, 2151–2163.
Ryugo, D.K. (**1992**). ''The auditory nerve: Peripheral innervation, cell body morphology, and central projections,'' in *The Mammalian Auditory Pathway: Neuroanatomy*, edited by D.B. Webster, A.N. Popper, and R.R. Fay (Springer-Verlag, New York), pp. 23–65.
Sachs, M.B., and Kiang, N.Y.S. (**1968**). ''Two-tone inhibition in auditory-nerve fibers,'' J. Acoust. Soc. Am. **43**, 1120–1128.
Sachs, M.B., and Abbas, P.J. (**1974**). ''Rate versus level functions for auditory nerve fibers in cats: Tone burst stimuli,'' J. Acoust. Soc. Am. **56**, 1835–1847.
Schneider, B.A., and Parker, S. (**1987**). ''Intensity discrimination and loudness for tones in notched noise,'' Percept. Psychophys. **41**, 253–261.
Schroder, A.C., Viemeister, N.F., and Nelson, D.A. (**1994**). ''Intensity discrimination in normal-hearing and hearing-impaired listeners,'' J. Acoust. Soc. Am. **96**, 2683–2693.
Siebert, W.M. (**1965**). ''Some implications of the stochastic behavior of primary auditory neurons,'' Kybernetik **2**, 206–215.
Siebert, W.M. (**1968**). ''Stimulus transformations in the peripheral auditory system,'' in *Recognizing Patterns*, edited by P.A. Kolers and M. Eden (MIT Press, Cambridge, MA), pp. 104–133.
Siebert, W.M. (**1970**). ''Frequency discrimination in the auditory system: Place or periodicity mechanisms?,'' Proc. IEEE **58**, 723–730.
Snyder, D.L., and Miller, M.I. (**1991**). *Random Point Processes in Time and Space* (Springer Verlag, New York), Chap. 2.
Steinberg, J.C., and Gardner, M.B. (**1937**). ''The dependence of hearing impairment on sound intensity,'' J. Acoust. Soc. Am. **9**, 11–23.
Stevens, S.S., and Davis, H. (**1936**). ''Psychophysiological Acoustics: Pitch and Loudness,'' J. Acoust. Soc. Am. **8**, 1–13.
Teich, M.C., and Lachs, G. (**1979**). ''A neural-counting model incorporating refractoriness and spread of excitation. I. Application to intensity discrimination,'' J. Acoust. Soc. Am. **66**, 1738–1749.
van Trees, H.L. (**1968**). *Detection, Estimation, and Modulation Theory: Part I* (Wiley, New York), Chap. 2.
Viemeister, N.F. (**1974**). ''Intensity discrimination of noise in the presence of band-reject noise,'' J. Acoust. Soc. Am. **56**, 1594–1600.
Viemeister, N.F. (**1983**). ''Auditory intensity discrimination at high frequencies in the presence of noise,'' Science **221**, 1206–1208.
Viemeister, N.F. (**1988a**). ''Psychophysical aspects of auditory intensity coding,'' in *Auditory Function: Neurobiological Bases of Hearing*, edited by G.M. Edelman, W.E. Gall, and W.M. Cowan (Wiley, New York), pp. 213–241.
Viemeister, N.F. (**1988b**). ''Intensity coding and the dynamic range problem,'' Hear. Res. **34**, 267–274.
Viemeister, N.F., and Bacon, S.P. (**1988**). ''Intensity discrimination, increment detection, and magnitude estimation for 1-kHz tones,'' J. Acoust. Soc. Am. **84**, 172–178.
Whitfield, I.C. (**1967**). *The Auditory Pathway* (Arnold, London).
Winslow, R.L., Barta, P.E., and Sachs, M.B. (**1987**). ''Rate coding in the auditory nerve,'' in *Auditory Processing of Complex Sounds*, edited by W.A. Yost and C.S. Watson (Erlbaum, New York), pp. 212–224.
Winslow, R.L., and Sachs, M.B. (**1988**). ''Single-tone intensity discrimination based on auditory-nerve rate responses in backgrounds of quiet, noise, and with stimulation of the crossed olivocochlear bundle,'' Hear. Res. **35**, 165–190.
Winter, I.M., and Palmer, A.R. (**1991**). ''Intensity coding in low-frequency auditory-nerve fibers of the guinea pig,'' J. Acoust. Soc. Am. **90**, 1958–1967.
Yates, G.K. (**1995**). ''Cochlear structure and function,'' in *Hearing*, edited by B.C.J. Moore (Academic, New York), pp. 41–74.
Yin, T.C.T., and Chan, J.C.K. (**1990**). ''Interaural time sensitivity in medial superior olive of cat,'' J. Neurophysiol. **64**, 465–488.
Yin, T.C.T. Chan, J.C.K., and Carney, L.H. (**1987**). ''Effects of interaural time delays of noise stimuli on low-frequency cells in the cat's inferior colliculus. III. Evidence for cross-correlation,'' J. Neurophysiol. **58**, 562–583.
Young, E.D. (**1984**). ''Response characteristics of neurons of the cochlear nuclei,'' in *Hearing Science*, edited by C.I. Berlin (College Hill Press, San Diego), pp. 423–460.
Young, E.D., and Barta, P.E. (**1986**). ''Rate responses of auditory-nerve fibers to tones in noise near masked threshold,'' J. Acoust. Soc. Am. **79**, 426–442.